Volume 8, Number 2 September 2010 ISSN 1881-4581

Journal of
eHealth Technology and Application

Supported by ITU-D SG-2 Q14

Published by Tokai University

Journal of eHealth Technology and Application

Special issue dedicated to

Digital Pathology for eHealth

and

Special issue dedicated to

Intelligent Systems for Biomedical Applications

Editor-in-Chief

Isao Nakajima, M.D., Ph.D., Ph.D.
Professor of Emergency and Clinical Crae
Director of Telemedicine & eHealth
Tokai University School of Medicine, Shimokasuya 143, Isehara
Kanagawa, 259-1143 Japan
Tel: + 81-463-91-3130; Fax: + 81-463-91-0780
E-mail: js2nb@ets8.jp

Chief Editor of the Special Issue

Yukako Yagi, Ph.D.
Director of the MGH Pathology Imaging & Communication (PICT) Center
Pathology Service
Massachusetts General Hospital
Assistant Professor of Pathology
Harvard Medical School
101 Merrimac St. Suite 854
Boston, MA 02114

Andriyan Bayu Suksmono, Ph.D.

Professor of School of Electrical Engineering and Informatics
Institut Teknologi Bandung, Indonesia.
Tel : + 6 2 – 2 2 – 2 5 0 1 6 6 1
Fax : + 6 2 – 2 2 – 2 5 3 4 1 3 3
E – mail : ab_suksmono@ltrgm.ee.itb.ac.id

Article adoption conditions are as follows;

1. All scientific papers (original articles) are peer reviewed by above-listed specialists.
2. Brief communication are selected by the Editors-in-Chief as a technical paper.
3. From the standpoint of the international policy, the Rapporteur of the Q14(ITU-D SG2 telecommunications for eHealth) can request the author to contribute her/his article to the report of ITU-D. In that case, another Copyright Assignment Agreement for the ITU publication has to be assigned separately from this Journal.

Sponsored by

KDDI

Journal of eHealth Technology and Application
Volume 8, Number 2
September 2010
ISSN : 1881-4581

EDITOR: ISAO NAKAJIMA, M.D., Ph.D., Ph.D.

Professor of Emergency and Critical Care
Director of Telemedicine & eHealth
Tokai University School of Medicine
Shimokasuya 143, Isehara-shi
Kanagawa, 259-1143 Japan
Tel: +81-463-91-3130
Fax: +81-463-91-0780
E-mail: jh1rnz@aol.com

Foreword

Yukako Yagi, Ph.D.
Department of Pathology, Harvard Medical School
Pathology Service, Massachusetts General Hospital, Boston, MA, USA

Digital Pathology is a relatively new field in medicine and still developing stage for clinical use. However, it is certain that pathology practice is going to be the image based with a computer's support like radiology.

After the Whole Slide Imaging Robot became available to produce virtual slides automatically, rapidly and a high resolution in late 1990s, many issues and limitations we had with telepathology and pathology imaging seemed to be solved.
But we had to face many other unexpected issues to use it in the clinical environment, for example the scanning speed and viewing speed are still slower than microscope based and have consistent image quality is not easy.
Last 10 years, people working on the Digital Pathology always think about the following items and made significant progress like the publications in this journal.

1. Speed
2. Reliability and consistency
3. QC of image quality and color
4. Management
5. Additional functions which microscope can not do such as Image Analysis
6. Workflow
7. Standardization

The WSI could dramatically change the telepathology for developing countries and rural areas. The combination of the WSI and Image Analysis can do diagnose and/or score from anywhere in the world about the cases in any other region in the world. Countries or institutions where no or few pathologists exist could have a big benefit through the technologies.
Recently, we have started WSI teleconference between developing countries. The cases we received before the WSI had low quality and limited number of images. Now we are more comfortable to give our opinions to them.

The data size of Digital Pathology is much larger than even radiology. It is challenging to manage and use the data effectively and it requirs wide range of the technologies such as computer, network, optics, data management, imaging, mechanics as well as pathology.
It is very important to work with an international organization such as WHO and/or ITU to make sure if all necessary standard protocol and regulation are placed.

Therefore, the publications in this journal contribute the new horizon to e-Health.

Preface

Mitra Djamal, Tati L.R. Mengko, Andriyan B. Suksmono; Guest Editors in Chief, JETA

This special issue contains a selection of interesting contribution from academia. In the first article, *Voice Spectrum Analysis and Fundamental Frequency Determination of normal, electrolarynx and Esophageal voice of Laryngectomiced Patients*, T.A. Sardjono, R. Hidayati, N. Purnami, A. Noortjahja, G.J. Verkerke, and M.H. Purnomo describe the speech spectrum analysis resulted from the normal voice and Indonesian laryngectomised patient with and without electro larynx. The voice will be recorded and analyzed using a spectrum analysis application to know the fundamental frequency. Laryngectomiced patient was operated to totally remove the larynx in order to clear out laryngeal cancer. The patient no longer breathes through its mouth but through a hole in his neck. This drastic change in the human body causes a loss of the ability of speech for the patient. Patient will learn to speech using esophageal speech or using an electro-larynx. The result shows that the fundamental frequency of 'a' and 'b' sound from laryngectomiced patient using an electrolarynx are 94 Hz and 102 Hz, respectively. It is hope that this result can be used to develop a new electronic voice producing element with an appropriate voice based on each human voice characteristics.

The second article, *Shape Transformation Using Grid Approach for Classification of X-ray Image*, Bertalya and Prihandoko propose a new method to classify X-ray images. Due to the many variations of object shapes obtained from object segmentation, they simplify the shapes by transforming detail shapes to global shapes. This transformation is implemented using a new approach, i.e. a grid approach. Euclidean Distance, Kullback-Leibler Divergence and Jeffrey Divergence techniques are used to obtain image similarity. Performance of this method is evaluated by calculating the recognition rate. The method gives high recognition rate. The recognition rate is 66% without shape transformation, but increases significantly to 83% with shape transformation.

The third article, *Fuzzy Logic Approach on Fatigue Classification due to Nine Hours Learning Task Based on Eye Movement Parameter*, Z. Arief, D. Purwanto, D. Pramadihanto, T. Sato and K. Minato describe a simple method for classifying the condition of fatigue, which is represented by morning and afternoon measurement of stimulated eye movement. Twenty-six visually normal students eye movement were examined and extracted to obtain their features or parameters, which are saccadic latency, velocity, saccadic duration, and deviation. Fuzzy based classifier is implemented for fatigue discrimination. Fuzzy membership functions are generated using the extracted eye movement parameters. The result reflected that the ocular muscles are directly affected by the fatigue. However, only the velocity and duration parameters shows significant difference ($p<0.05$) between fatigue and nonfatigue condition.

In the fourth article, *Analysis the Dominant Location of Brain Activated in Frontal Lobe during Activities Using K-means Method*, Kemalasari and M. H. Purnomo analyse EEG signals to determine the dominant locations of brain activated in the frontal lobe during activities using K-means methods. BIOPAC MP 30 is used to measure EEG signals during activities. The kind of activities are listening to Al-Qur'an, reading Al-Qur'an, listening to music, relax, solving mathematic question, and solving puzzle. K-means method is used to determine the dominant location of brain activated in frontal lobe. The result of this research is the location of brain activated during listening to Al-Qur'an, reading Al-Qur'an, listening to music and relax condition seems to be in the right of frontal lobe. The error grouping level of the dominant location of brain activated by K-Means method is 0 % during relax condition, 7.1 % during listening to Al-Qur'an and solving puzzle conditions, 14 % during reading Al-Qur'an and solving mathematic question conditions, and 21 % during listening to music condition.

In the fifth article, *Brain-Inspired Knowledge-Growing System and Its Application in Biomedical Engineering: Inferring Genes Behavior in Genetic Regulatory System*, A.D.W.

Sumari, A.S. Ahmad, A.I. Wuryandari and J. Sembiring use concept of Brain-inspired Knowledge-Growing System (KGS) for inferring the behavior of genes interaction in a Genetic Regulatory System (GRS) in order to estimate its behavior in the subsequent interaction times. For this purpose they model the genes as multi-agent that performs collaborative computations in Multiagent Collaborative Computation (MCC) paradigm. In order to show how KGS works in MCC framework, they use yeast25 genes-interaction values as the case study. From the knowledge obtained by KGS, they can make estimations regarding the expressiveness of individual gene and all genes behavior during a certain cycle of genes interaction.

Finally, in the last article, *Robotic and Telematic Assistant Technologies to Support Aging People*, Daniel Eck and Klaus Schilling introduce assistive technologies to support a self-determined living of elderly people. In this context robotic and sensoric approaches can balance handicaps to improve safe mobility approaches. By telematic methods health data can be transmitted to enable a continuous monitoring of endangered people in their home or while travelling. Thus assistant technologies will support an independent living of elderly people in their used environment without missing the quick support by medical services.

I sincerely hope this issue will enable us to continue meeting the expectations of our readers and contributors.
Finally, once again, I thank all the contributors for publishing through this journal.

Mitra Djamal (Professor, Faculty of Mathematics and Natural Sciences)
Tati Latifah R. Mengko (Professor, School of Electrical Engineering and Informatics)
Andriyan Bayu Suksmono (Professor, School of Electrical Engineering and Informatics)
Institut Teknologi Bandung
Jl. Ganesha No.10, Bandung,
Indonesia

Journal of eHealth Technology and Application

Volume 8 Number 2 September 2010

I: Special issue on Digital Pathology for eHealth

II: Special issue on Intelligent Systems for Biomedical Applications

III: Original Articles

I: Digital Pathology for eHealth

Digital Pathology from the Past to the Future

Yukako Yagi, John R Gilbertson

Harvard Medical School

Introduction: The rise of the whole slide imaging robots

The ability to digitize histopathology slides automatically, rapidly and a high resolution has been advanced by numerous investigators around the world over the past approximately fifteen years. The goal of these introductory paragraphs is not to record the history of this accomplishment in detail, but provide a series of markers so that future development can be estimated. While the first attempt at "whole slide imaging" is hard to determine, the conversion at Nikon Labs in the early 1990s of 35 mm and 3x4 film digitizers into devices for low resolution scanning of glass histology slides [1] [2] is close to the beginning. Prior to this time, commonly available computers simply did not have the capacity to handle a "digital slide'" in a meaningful way.

In 1997, Dr Joel Saltz and his group at Johns Hopkins and the University of Maryland published work on prototype "Virtual Microscope". Though it did not appear to image entire slide, it did digitize large areas of slides at high resolution and had many of the attributes of modern whole slide imaging devices. The group's 1997 [3] and 1998 [4] papers discuss the limitations of the device, the limitations of current technology in supporting the robotics, data management, data storage and data distribution inherent in high resolution, wide field, slide imaging and discuss many of the issues that are still central to whole slide imaging today.

By 1999-2001 however, generally available computer technology began to catch up the needs of whole slide imaging and small companies such as Interscope (Pennsylvania) and Aperio (California) began developing and marketing devices that had all of the features of modern whole slide imagers. The authors had personal involvement with the early Interscope device and therefore can discuss its parameters. The device was based on a digital video camera and a high end, 1999, personal computer (storage was limited and supplemented by additional devices). The optics provides a 20x magnification and the CCD's 6.6 um square pixels provide a spatial sampling period on the tissue of 0.33 um/pixel. The camera was synchronized with a strobe light (for illumination) and both were synchronized with stage motion through a set of optical rulers mounted on the fixed and moving parts of the stage. Tissue finding and focusing was separate from high resolution scanning. Tissue finding was done through a separate relatively low resolution snapshot camera. From the snapshot image, the system identified a set of tissue points for autofocus and that data was used to guide the objective lens during the high speed, high resolution scan. The scanning phase for a 1.5 cm tissue section took 15 to 8 minutes (depending on the model) at 20x.

From 2000 to today, a large number of small and large companies have contributed to the development of modern whole slide imaging technology. There is a wide range of devices available for a wide range of purposes; however, a high end, general use scanner today will accept a batch of bar coded slides and image them at 40x (spatial sampling of ~ 0.15 um/pixel) in about one minute per slide including all slide handling, focusing and scanning.

Going forward, we expect that the field will continue to evolve. In this paper, we will discuss the fundamental "grand challenges" intrinsic to whole slide imaging (things like file size, interactivity and image quality) and well as operational challenges that are developing as the use of digital slides used in clinical labs (things like validation and quality control, data and communications standards as well as the relationship between whole slide imaging and the clinical histopathology laboratory). We discuss the current accepted use of digital slides and, finally, what needs to happen for large scale whole slide imaging to become a compelling business case for the typical pathology practice.

Grand technical challenges

Management of large image files, the need for highly interactive display of these images, and fast, reliable image capture remain grand technical challenges. These will be solved, either through direct innovation or by the continuous improvements in the general computation, storage, robotics and network markets; however, for near term they will continue to create significant technical, infrastructure and financial headwinds to the large scale implementation of digital pathology imaging systems.

File Size: A typical, stained microscope slide contains a large amount of potential data. The normal surgical

pathologist uses a microscope which a variety of objectives, the most powerful of which is usually a high corrected, 40x lens with an numerical aperture of approximately 0.9. While the pathologist never scans the entire slide at 40x, very few pathologist are willing to give up their 40x lens because it is necessary, in a variety of common diagnostic situations, to examine small areas of the slide at that magnification.
In the whole slide imaging paradigm the pathologists loses control of the sampling process (the machine, not the pathologist, determines what part of the slide is digitized and at what magnification), this means that the entire slides (or at least, all of the tissue on the slide) needs to be imaged at 40x. While some (including the authors of this review) have argued (and demonstrated) [5] that many cases can be successfully handled at maximum magnification of 20x, we know of no controlled studies in which pathologists have removed the 40x lens from their microscopes and compared their results (and their confidence) with a group who retained the 40x lens. For this reason, and because 40x scanning is becoming increasingly available in commercial systems, the scanning slides at 40x is a reasonable place to begin a discussion on file size and its implications.

Given a common CCD with six micron pixels and a 40x optical magnification of the tissue, each pixel will subtend a square of tissue 0.15 um along each side (this is consistent with the specifications of most 40x scanners today). This results in 4.4 billions pixels per square centimeter. With 24 bit RGB color, this is approximately 13 GB per square centimeter. Taking the conservative assumption that one square centimeter is the area of tissue on a typical slide and that the "white areas" can be either ignored or compressed to insignificance, this is still a substantial amount of data. A large academic medical center such as the Massachusetts General Hospital generates ~ 2500 slides per day. At 13 GB per slide this is 32,000 GB daily. A 30:1 JP2000 compression could potentially decrease this to 1 TB/day, while the potential capture of more than one focal plan or the use of multispectral technology will increase it.

The major implication of file size to the challenge of large scale digital imaging in pathology is what it does to infrastructure, interactively and cost; as will be discussed below.

Interactivity: Traditional medical imaging systems and Picture Archive and Communications Systems (PACS) operate on the principle of exchanging full image files between devices [6]. If a workstation requests a CT study, the entire study is sent to the workstation which then manages it and displays it locally. The size of high resolution whole slide images makes this model impracticably in digital pathology. Since their earliest development in the late 1990s, whole slide imaging systems have used a client-server system in which image files are structured as multi-layered "pyramids" where the base of the pyramid is the high resolution image, the middle layers are lower resolution images (created by the system by sub-sampling the high resolution image) and the apex is a whole slide thumbnail. Each layer is divided into equally sized tiles and it is these tiles that are sent to the client on demand. Very much like a "Google Maps" application, the majority if the data in a digital slide stays in the server and it is the pathologist's panning and zooming requests that determine which tiles are sent across the network to the client (panning or zooming cause the client to request the appropriate tiles from the server which in turn sends the appropriate tiles back to client). While this approach does allow the pathologist access to the digital slide without waiting for the entire data set to download (and careful network design can improve performance [7], it also means that panning and zooming is slower than it would be than if the data set was local; and, significantly, it is much slower than the response time when a pathologist moves a physical slide on a microscope stage. This slower interaction more than cancels any time saved by the wider field of view (at low magnification) seen in most digital slide systems and is the root cause of the comment, seen in virtually all papers on the diagnostic use of WSI [8], that it takes longer to review a case through the computer than does when the physical slides are available in a microscope.

Slide variances from the histology lab: In the early development of whole slide imaging (and until fairly recently), digitizing the slide was considered a very different process from creating the slide. Most papers evaluating digital slides for diagnosis used "standard" slides made in a "standard" way. Only recently has the been much discussion on how the way the slide is made impacts the way it is digitized and the quality of that digital image [9].

If tissue sections were perfect, if they were square, flat and parallel to the slide (and if the slide was flat and square), if the tissue sections were located at predictable location on the slide, if the cover-slip was well placed, if there were no tissue folds or bubbles and if there was little or no variance between slides – digitizing slides would be much, much easier. Unfortunately, a tissue section is incredibly delicate and slide making in most histopathology labs is a highly manual process done, by skilled people, under a significant level of time pressure. Furthermore, the eyes of the pathologist can see through or around most of the variances that this manual, high pressure system necessarily creates. It is not as easy for the whole slide imaging robot. WSI designers have had to incorporate complex focusing, tissue finding and slide handling mechanisms to get around slide, tissue and stain variances. These mechanisms increase capture time (as well as device cost), yet do not completely solve the problem. In our experience, and that of the literature [10], a large (but decreasing) percentage of images (approximately 3-5%) need to be re-scanned because large areas are out of focus, some parts of the issue were not 'found' (not imaged) or because the slide gets

'stuck' or gets involved with another type of slide handling mis-adventure. Furthermore, if one looks hard enough, one can fine small areas of less than optimal focus in virtually every digital slide [5]. While small areas are easy for pathologist to read around, when small areas of poor focus overlap small, areas critical for diagnosis, problems can occur [5].

There is another issue in the histology lab that impacts the large scale use of whole slide imaging: the use of large batch processing [11]. In many laboratories (though the practice is decreasing), the case received the day before are processed overnight. Slide are made and stained in the early the next morning so that slides are available to the pathologist by mid morning. This practice puts pressure on the laboratory to get slides out quickly and creates relatively large batches of slides in the mid morning and, by extension, makes it much more difficult for laboratories to implement whole slide imaging. No matter how fast a device is, it will take a significant period of time to digitize a large batch of slides; and if that time is during the most critical part of the day (mid-morning when the pathologists are waiting for their slides), it will be very difficult to convince a practice to incorporate large scale pre-diagnostic digitization.

Fortunately, there are two trends in the histology lab that should, over time, mitigate this problem. The first is the use of automated histology robotics. The machines are available to automate virtually every step of the slide making process including processing, embedding, staining and cover-slipping. Even automated tissue sectioning is becoming available. These devices should help decrease slide variances and should therefore improve digital image quality. These devices also can be run in mini-batch or continuous flow modes. In these modes, specimens are placed in the process almost as soon as they are received and grossed and the tissue moves through the laboratory in a continuous, assembly line like way. Not only does continuous flow provide a higher throughput (which usually means getting the slides to the pathologist faster), it also means that the lab is producing slides at rate on the order of one slide per minute on continuous basis. It would not be unreasonable to consider placing a fast (less than a minute) slide scanner at the end of the process. This would allow virtually all slides to be imaged, pre-diagnostically, with virtually no impact on the laboratories throughput or the pathologist's schedule.

Image Quality: Image quality is obvious goal, but one that has been remarkably difficult to define. Image quality can involve, most basically, image capture; but it also can modified during post capture processing (i.e. compression) as well as at display. Even the ambient light in the pathology's office can affect the perception of the image [12]. For the purpose of putting scope around this discussion, we will focus on image capture and specifically on tissue finding, focus and depth of field.

Tissue finding is a very important step in the imaging process. Because the tissue area (the area of the slide which contains tissue) is usually much smaller than the total glass or cover-slip area, many whole slide imaging systems attempt to improve scanning times by identify the tissue on the slide in a rapid, low resolution snapshot. The tissue areas identified are then scanned at high resolution. While simple in theory, this is sometimes difficult in practice. Tissue fragments can be small, under or over stained and can look remarkably like dirt, grease or cover-slip edges at low resolution. Most importantly, failure to identify (and by extension, failure to image) an area of tissue can be catastrophic if the area has unique, critical diagnostic information. Failure to present all the tissue to the pathologist will result in a lack of confidence in the system and would be a major barrier to large scale, clinical implementation. Failure in tissue finding is most significant not in teaching or in second opinion scenarios, but in potential "primary diagnoses" from digital slides in which no pathologist would see the glass slides directly. While systems have gotten much better at tissue finding in recent years, in our current experience, this still remains an important issue in many situations.

Focus remains the most important issue in whole slide imaging. While with careful quality assurance, careful, competent technicians and careful pathologist major diagnostic error due to focusing error can be minimized, it remains an area of concern as careful examination of digital slides routinely show small areas of less than optimal focus, and though pathologist can usually read around these artifacts, it is not reasonable to expect the pathology community to accept a technology that provides more artifacts (in the form of areas of poor focus) than the current gold standard (the direct examination of the physical slide on the microscope). Like tissue finding, focus is something that is taken out of the pathologist's hands in an automated whole slide imaging environment and the systems must be able to provide a very capable substitute. Increasingly devices are incorporating more focusing points and even real time focus; this, and lower variance in slides from the histology laboratory, should result in increasingly better focus in the years ahead.

Related to focus is the issue of depth of field or multiple focal planes. High numerical aperture lenses (such 0.9 NA 40x objectives) have depth of fields that are significantly smaller (thinner) that the tissue sections being examined. This means that even of a tissue section is in focus, parts of the tissue section (above and below the level in focus) will not be in focus. The importance of this depends on the diagnostic question in play, but, because do not control focus in current imaging systems, at high numerical apertures, pathologist using a WSI system has potentially access to less of the tissue section than a pathologist using a microscope. While we can

image that future device will have different optics, or scan multiple focal planes, and thereby mitigate this issue. This may likely happen at the cost of larger image files and more complicated interactivity.

The grand technical challenges, technology, infrastructure and cost:

The challenges above show both promise and concern for the large scale use of digital slides. With the exception of tissue finding and focus, which are intrinsic to the whole slide imaging device and will almost certainly be solved by advance of technology, the challenges involve issues of infrastructure and cost. While it is true that the cost (and the availability) of computational power, network connectivity and storage space will continue to improve which general improvements in technology, and that there will be a time at which, even if pathology does nothing, the cheap storage, fast networks and advance robots needed to meet the challenge of large scale, pre-diagnostic whole slide imaging will be available as part of the general hospital infrastructure. On the other hand, getting ahead of the technology curve – building storage and network infrastructure that is ahead of what is generally available - is expensive and will have to compete for funding with other initiatives in pathology and across the hospital. It is very important therefore to the near term implementation of WSI, that digital pathology be developed in a way that decreases costs and improves capability / service for pathology practices, and does so in a more convincing way than other potential capital investments (vide infra: the core of a business case).

System Testing, Quality Control and Validation

In addition to the technical challenges discussed above, pathology faces a number of operational challenges in the large scale use of digital slides. These can be discussed in three main areas: system validation and testing, data and communications standards and LIS involvement

Validation, for this discussion, can be divided into separate though related parts, the validation that the clinical laboratory needs to do, on a regular basis, to make sure that imaging systems are working appropriately (technical validation) and validation that companies, governmental agencies and pathology organization might do to compare the diagnostic capabilities of digital slide systems with traditional microscopes.

Technical validation and testing in histology: The creation and use of a digital slide is surprising complex. Unlike radiology, in histopathology, the image is not created when photons hit a CCD. In pathology the creation of an image is physio-chemical process in tissue that involves fixation, processing, embedding, cutting, staining and even cover slipping. The details of the histology process is well beyond the scope of the article [13], but there is little doubt that variations in histology practices (and slide to slide variances within the same process) have significant impact on image quality. For example, variation in staining intensity can result in tissue finding errors, a focus point on a fold or bubble can result in local lack of focus, thickness of tissue section can affect image quality and poor cover-slipping can result in serious slide handling errors [8]. Unfortunately, histology laboratories do not have extensive, quantitative parameters for quality assurance. In most places, the pathologist is the ultimate "customer" and his or her holds sway.

It is interesting that whole slide imaging itself may hold the key to a virtuous quality feedback loop: the digital data in whole slide images, combined with image analysis programs, may generate quantitative histology quality assurance information which could improve slide quality and, by extension, whole slide imaging quality. An example how this might work is shown in Bautista et al in their work on quantitative analysis of tissue folds [14].

Technical validation and of color fidelity: Fidelity of color is important in digital imaging systems. While it is no doubt true that pathologists easily read through variations in stain saturation on slide under the microscope, and that there are numerous outstanding pathologist who happen to be color blind; it is also true that digital systems can allow large, unexpected changes in the color displayed, and changes in color can effect contrast and resolution (two adjacent green pixels cannot be resolved). While there are international standards in the digital communication of color [15], not all pathology systems support these standards, more importantly, color information will be 'handed off' between systems numerous times in pathology practice (the scanner, the compression board, the server, the workstation, the view software, the monitor, etc). The pathologist needs a way to insure that the color displayed on the screen is the true color observed on the specimen [16].

A simple solution to this problem is the Yagi adaptation of the MacBeth color chart for microscopic imaging [17]. The original MacBeth Color Checker is an array of 24 squares, each a different color, that is used for precise color balance in general digital photography. The Yagi adaption uses an array of nine color filters on a microscope slide which can be scanned by a whole slide imaging device. This image displayed on a remote monitor (on a pathologist's desktop) can be compared with a local copy to assure that the color balance is correct.

Technical validation and testing of focus and resolution: The technical validation of focus and resolution is challenging in the whole slide imaging environment. Because whole slide imaging robots are responsible for

creating a focused image (in other words, a pathologists presented with a whole slide image has no control over how it was focused), validation of the system's ability to this is extremely important. There are "calibration slides" which include calibration and resolution markers on them, but limited value because the optical and digital resolutions are seldom in doubt. What one needs is a measure of the system's ability to consistently focus a tissue which is floating, twisted, folded and puckered in three dimensional space.

In our laboratory, we measure and validate the focus by providing a "standard" slide of a mice embryo sectioned and stained in an automated histology system. A high quality scan is stored in the system and compared with validation runs (of the same slide) on a regular basis. The quality of the overall images is compared as well as specific fields in several of the organs.

Technical validation and testing of tissue finding: Failure to identify and scan all of the tissue on a slide one of the most serious failures for a whole slide imaging system. The main reason for such a failure is light staining of the tissue section (this is seen most often in IHC slides with light counter-stains). We have keep a set of slides that caused systems to fail tissue finding in the past, These are run on regular basis to make sure that the changes make to the system settings (to correct the tissue finding failure) are still working. The second approach is technical difficult and we have not yet developed it fully into a completely working system. The heart of the system is a slide with a set of small tissue sections each with various degrees of staining (from very dark to very light). To pass this test, a system must be able to find all tissue sections with a certain level of staining,

Comparison testing of whole slide imaging systems against the optical microscope: In the past year or two, there has been increased interest in validation of digital imaging systems against the optical microscope in the specific use case of primary pathology diagnosis. As will be discussed below in the section on "Acceptance of Digital Slides", the pathology profession is becoming increasing comfortable with the use of digital slides in teaching, quality assurance, second opinion consultation and remote frozen section, and published data in the literature indicates that the technology is safe and very useful especially in applications that involve long distances and some amount of time pressure.

The primary diagnosis paradigm is somewhat different from the other uses of whole slide imaging in that a case could potentially be signed out without ever being seen under the traditional optical microscope. There is concern in some quarters that the digital systems should be proven to be as good as the microscope before it is approved for use in primary diagnosis. Last year, the United States Food and Drug Administration opened a panel to examine this issue (on of the authors, JG, was on that panel). The panel has had a single introductory meeting and has not made a formal statement on the topic.

Here, we will only re-iterate what we have stated previously in the literature and in published guidelines such as the 1999 American Telemedicine Association Guideline for Telepathology [18]. The pathologist has a wide range of diagnostic tools at his disposal and it is the responsibility of the pathology to chose the right tool(s) for a given case and make sure that the data image quality coming from those tools is of appropriate quality for diagnosis (vide supra, technical validation). It has never been a question of which tool was better, but rather which tools are safe and useful. Furthermore, all tools are used in a diagnostic system and it the output of the system that really matters to the clinicians and patients. If digital systems are used in a way that changes the diagnostic workflow (for example, by allowing more consultation, more access to clinical data, more use of quantitative measures, etc) this should be considered in any evaluation.

Need for large scale, long term data collection: Several published studies in whole slide imaging and robotic microscopy indicate the likelihood that different specimen types and diseases are more or less amenable to digital slide analysis. For example Dr Wilbur and his colleagues [19] have mentioned inflammatory diseases as potentially more difficult to diagnosis on a digital slide; a comment backed up by previous work by Dr Dunn in his comments on the difficulties presented by inflammatory gastric cancer [20]. Long term database of difficult cases would certainly be useful to pathologists as they determine which tools are most useful for which cases.

Data and Communication Standards:

Created by the America College of Radiology and the National Electronics Manufacturers Association in the 1980s, DICOM (Digital Image COmmunication In Medicine) is the primary standards organization for the sharing of clinical images and related data for virtually all medical specialties, and forms the basis for inter-vendor connectivity in Picture Archiving and Communication System (PACS). DICOM works through public working groups, and in 2005, it created a new working group, working group 26, to incorporate pathology imaging into the existing standard and to propose extensions to the standard (known a supplements) as needed.

So far, Working Group 26 proposed to supplements. The first, Supplement 122, involved data about the specimen that is the subject of an image. Supplement 122 has been balloted, approved and is now part of the DICOM standard. It involves information about the specimen (that is the subject of an image) that is needed to interpret that image [21]. An example of this information

would be how the specimen (the tissue section) was stained. Supplement 122 (as well as the entire DICOM standard, working group minutes, schedules and how to join the working group) is available on the internet at http://medical.nema.org.

The second supplement (Supplement 145) is currently being balloted. Supplement 145 proposes how whole slide image files can be shared in DICOM, and deals with a number of difficult issues including the large file size, its pyramid structure and the way it is exchanged as a set of semi-independent "tiles" (vide supra). Should 145 be approved and become part of DICOM, scanner makers, PACS vendors, workstations will be able to build to a shared standard, and pathology departments that purchase DICOM compliant systems) will have a standard way of sharing whole slide images.

The incorporation of the LIS, the Histology Department and Imaging

Until very recently, in the great majority of situations, imaging has been looked at separately from the histology lab and the Laboratory Information System (LIS). This is sub-optimal. As discussed above, in pathology, images begin in histology and problems seen by whole slide imaging systems (such as tissue finding, focus, etc) often find their root cause in histology activities. Increasingly, pathologists are looking at whole slide imagers as another automated device in an increasingly automated histology process.

In the same way, ordering an image should become more incorporated in the pathology workflow (as supported by the LIS). Currently, LIS systems support histology protocols on the basis of specimen type (for example, at the accession of a colon biopsy from screening colonoscopy, the LIS might create default orders for one block and three stepped slides, each stained with H&E). We can expect, in the future, that the LIS might also order imaging and perhaps several image analyses on the slides. In a somewhat simpler example, a pathologist ordering a quantitative image analysis on a special stain need at the same time to order the slide and the stain. Imaging and histology are joined at the hip and need to be though of as a single system.

Current Acceptance of Digital Slides

While full clinical use (pre-diagnostic imaging of all slides) is the long term goal of research laboratories and the industry in general, whole slide imaging has already been accepted at various levels of pathology practice. This step wise acceptance is based on the scale (number of slides involved), the time criticality and the image quality requirements of the levels involved.

Education and training: Following the initial (and continuing) work of Dr Dee (University of Iowa) [22] [23] and others, in medical school training in histology and pathology whole slide imaging is the standard practice across the country. There are a number of reasons for this, including ease of use by students, 24x7 and out of class room access, the ability to incorporate annotation and testing, the ability of the class to share a single digital slide (as opposed to the need to support multiple physical slide boxes) and the cost of microscope maintenance and storage. Digital slide based coursed are simply better accepted, cost less to produce and seem to have better educational results. Significantly, over the past couple of years, we are seeing more and more pathology residency candidates asking specifically if our residency program supports digital slides.

At residency, programs increasingly are supporting digital training sets (managed by the department or, more often, but the residents themselves). Slides for teaching conferences are often digitized and US national pathology boards have recently become fully digital. There has been a slow implementation of digital slides in clinical conferences (tumor boards) and on specialty web sites.

Finally, there is an increasing interest in the use of whole slide images and structured data entry in simulation based teaching (and testing) [24]. The basic idea is to take an area of pathology, such as frozen section diagnosis or prostate cancer, set up a collection of digital slides and gold standard, structured reports and let residents "signout" these cases in an digital environment that simulates real world practice. Just like in the airline industry, residents (or pilots) are tested in simulation before they get to the real world.

Workflow and documentation: Another area of development in whole slide imaging is the use of the technology to document rare slides or slides that cannot be retained by the practice. The most common situation is a consultation practice that must return slides to the referring practice but still wants to document the morphology that was the basis of the consultation report. In many cases, the consulting practice is a academic medical center or cancer center and the patient is often sent to that center after the consultation (meanwhile, the slides have been sent back to the referring hospital). This application is well suited for the current generation of scanners because it involves a limited, well defined set of slides and the imaging is done after the diagnosis is rendered, making capture speed and throughput less of issue.

Tele-pathology: The purpose of this discussion, we will define tele-pathology as the spatial separation of the slides from the location where the slides are interpreted. A variety of practices fit this general definition.

Several practices and at least one reference laboratory use telepathology to share immunohistochemistry slides from the laboratory to the pathologist in the fastest way

possible. The reference laboratory, US Labs (http://www.uslabs.net/) has a "virtual laboratory" component which provides technical services (as opposed to formal diagnostic reports) to, largely, community pathologists. The pathologists send tissue blocks or unstained slides to the lab and the lab does the staining and send the stained slide back to the pathologist both physically (through a courier service) and as a digital slide (through the internet from their server). The digital slide is often acceptable to the pathologist and allows for a faster turnaround time.

Remote frozen section support is another current use of whole slide imaging. Several large, published series [25] [26] have shown that at least in neuropathology, whole slide imaging, when well validated and controlled, can be used successful to support frozen sections with very acceptable diagnostic accuracy and turn around times. Furthermore, it allows more pathologists to participate in difficult cases.

Another interesting and useful application of whole slide imaging is the support of a remote rapid breast diagnosis center in Arizona [27].

Primary diagnosis on digital slides: A key component of whole slide image based telepathology (as discussed above) is that, somewhere in the process, a pathologist's sees the physical slide under the microscope. In IHC distribution, the physical slide is also sent and the primary pathologist sees the H&E on glass. In second opinion consultation, the primary pathologist is directly examining the physical slide; even in the frozen section use case the diagnosis will be followed up by glass on microscope interpretation and difficult frozen sections can be deferred to permanents. The Dr Dunn's VA model is a robotic microscope model (not a whole slide imaging model) in which the pathology has robotic control of focus and can examine the entire slide; however indicates that primary diagnoses can be successfully made, remotely and on a computer screen, over long periods of time [28].

The authors know of no published situation in which primary clinical diagnosis was done exclusively by digital slides. There is a number of digital slide – glass slide equivalence studies in the literature, but are relatively small studies. In the fall of 2009, the US Food and Drug Administration set up a panel to examine the use of automated whole slide imaging in primary clinical diagnosis but the panel has had a single information gathering meeting and has made no announcements.

The Core of a Business Case

The Core of a Clinical Business Case

In this paper we have reviewed the rapid advance of whole slide imaging and digital slide technology as well as the major challenges that it faces as moves from a largely education and research application to mainstream clinical application involving large numbers of clinical slides. From the existing literature and the record of development to date, there is a compelling, if not completely proven, argument that current whole slide technology is capable of reliable, diagnostic quality images and that quality will improve further with better focus technology and the speed needed to routinely image multiple focal planes.

That said, it is also clear that large scale implementation of whole slide imaging and digital slide technology will be expensive, especially in the near term, when it comes to the changes infrastructure that will be needed by most practices, and it must be remembered that digital pathology will have to compete with other compelling laboratory initiatives for the limited capital funds of pathology practices.

Digital slides should be able to create enough efficiency or capability for a practice so that is can generate a return large enough to successfully compete for funding. It will do this based on the fundamental advantages of digitization in the modern world: the ability to apply computational power and network connectivity. For anatomic pathology, this means diagnostic image analysis and tele-pathology (the ability to separate the location of the slide from the location of the interpretation).

For image analysis to become a driving force for the wide spread use of digital slides it must provide highly useful capabilities that could not be obtained any other way. While there is almost no doubt that a combination of special stains, illumination (for example, multi-spectral imaging), and computational analysis will allow us to do very powerful things that we cannot possibly do now, including perhaps creation of intelligent pathologist assistance systems and new grading systems that better inform prognosis and better guide therapy, these things will require development of computational techniques, new markers (potentially) and the discovery of relationships between computational results, prognosis and outcomes – and this will take time.

Until that time, we expect that most instructions will do what our institution is doing, continue to develop and implement teaching applications, including simulation; establish an imaging research lab, set up a core pathology research facility to begin develop diagnostic applications of image analysis and multispectral imaging initially in research be ultimately in clinical practice; apply digital slides when useful in tele-pathology and quality assurance applications; upgrade the automation in our histology lab an establish the ability to run operations with continuous specimen flow; and, piece by piece, specimen type by specimen incorporate whole slide imaging and image analysis into our primary diagnosis clinical operations – all at the same time watching as the infrastructure costs (storage and

network) become increasingly affordable.

People began thinking seriously about whole slide imaging and digital slides about fifteen years ago. We expect widespread, routine clinical use of digital pathology fifteen years from now. It will be an interesting time.

References

[1] Azumi N, Yagi Y, Elsayed A, Mun S. Telepathology for the Masses: Formation of the "International Consortium of Internet Telepathology". Cell Vision. 1996; l3 (6): 447- 452

[2] Yagi Y, Azumi N, Elsayed AM, Mun S. Evaluation of Image Quality and Factor for International Telepathology through The Internet. Proceedings of SPIE, Medical Imaging, Image Display 1997:810 – 819

[3] Ferreira R, Moon B, Humphries J, Sussman A, Saltz J, Miller R, Demarzo A. The Virtual Microscope. Proc AMIA Annu Fall Symp. 1997:449-53.PMID: 9357666 [PubMed - indexed for MEDLINE]

[4] Afework A, Beynon MD, Bustamante F, Cho S, Demarzo A, Ferreira R, Miller R, Silberman M, Saltz J, Sussman A, Tsang H. Digital dynamic telepathology--the Virtual Microscope. Proc AMIA Symp. 1998:912-6.PMID: 9929351 [PubMed - indexed for MEDLINE

[5] Gilbertson JR, Ho J, Anthony L, Jukic DM, Yagi Y, Parwani AV. Primary histologic diagnosis using automated whole slide imaging: a validation study. BMC Clin Pathol. 2006 Apr 27;6:4.PMID: 16643664 [PubMed]

[6] Branstetter BF, editor. Practical Imaging Informatics: Foundations and Applications for PACS Professionals. Springer; 1st Edition (October 13, 2009): ISBN-10 1441904832

[7] Lundin M, Szymas J, Linder E, Beck H, de Wilde P, van Krieken H, García Rojo M, Moreno I, Ariza A, Tuzlali S, Dervişoğlu S, Helin H, Lehto VP, Lundin J. A European network for virtual microscopy--design, implementation and evaluation of performance. Virchows Arch. 2009 Apr;454(4):421-9. Epub 2009 Mar 12.PMID: 19280223 [PubMed - indexed for MEDLINE]

[8] Wilbur DC, Madi K, Colvin RB, Duncan LM, Faquin WC, Ferry JA, Frosch MP, Houser SL, Kradin RL, Lauwers GY, Louis DN, Mark EJ, Mino-Kenudson M, Misdraji J, Nielsen GP, Pitman MB, Rosenberg AE, Smith RN, Sohani AR, Stone JR, Tambouret RH, Wu CL, Young RH, Zembowicz A, Klietmann W. Whole-slide imaging digital pathology as a platform for teleconsultation: a pilot study using paired subspecialist correlations.Arch Pathol Lab Med. 2009 Dec;133(12):1949-53.PMID: 19961250 [PubMed - indexed for MEDLINE]

[9] Yagi Y, Gilbertson JR. A relationship between slide quality and image quality in whole slide imaging (WSI). Diagn Pathol. 2008 Jul 15;3 Suppl 1:S12.PMID: 18673500 [PubMed]

[10] Gilbertson JR, Ho J, Anthony L, Jukic DM, Yagi Y, Parwani AV. Primary histologic diagnosis using automated whole slide imaging: a validation study. BMC Clin Pathol. 2006 Apr 27;6:4.PMID: 16643664 [PubMed]

[11] Gilbertson J, Yagi Y. Histology, imaging and new diagnostic work-flows in pathology. Diagn Pathol. 2008 Jul 15;3 Suppl 1:S14.PMID: 18673502 [PubMed]

[12] Masahiro Yamaguchi, "Multiprimary Displays for natural color reproduction," Proceedings of the 2nd International Meeting on Information Display (IMID 02), (2002) 999-1004

[13] Kiernam JR., Histological and Histochemical Methods: Theory and Practice. Scion, 4th Edition (2008). ISBN 978 904842 42 2

[14] Bautista PA, Yagi Y. Detection of tissue folds in whole slide images. Conf Proc IEEE Eng Med Biol Soc. 2009;2009:3669-72. PMID: 19964807 [PubMed - indexed for MEDLINE]

[15] International Color Consortium; http://www.color.org

[16] Kayser K, Molnar B, Weinstein RS. Digital pathology virtual slidetechnology in tissue-based diagnosis, research and education. Berlin:VSV Interdisciplinary Medical Publishing; 2006. p. 1-193.

[17] Weinstein RS, Graham AR, Richter LC, Barker GP, Krupinski EA, Lopez AM, Erps KA, Bhattacharyya AK, Yagi Y, Gilbertson JR. Overview of telepathology, virtual microscopy, and whole slide imaging: prospects for the future. Hum Pathol. 2009 Aug;40(8):1057-69. Epub 2009 Jun 24.PMID: 19552937 [PubMed - indexed for MEDLINE]

[18] Available at the website of the American Telemedicine Association's web site at: http://www.americantelemed.org/files/public/standards/ClinicalGuidelinesForTelepathology_withCOVER.pdf.

[19] Wilbur DC, Madi K, Colvin RB, Duncan LM, Faquin WC, Ferry JA, Frosch MP, Houser SL, Kradin RL, Lauwers GY, Louis DN, Mark EJ, Mino-Kenudson M, Misdraji J, Nielsen GP, Pitman MB, Rosenberg AE, Smith RN, Sohani AR, Stone JR, Tambouret RH, Wu CL, Young RH, Zembowicz A, Klietmann W. Whole-slide imaging digital pathology as a platform for teleconsultation: a pilot study using paired subspecialist correlations. Arch Pathol Lab Med. 2009 Dec;133(12):1949-53.PMID: 19961250 [PubMed - indexed for MEDLINE]

[20] Dunn BE, Choi H, Almagro UA, Recla DL, Krupinski EA, Weinstein RS. Routine surgical telepathology in the Department of Veterans Affairs: experience-related improvements in pathologist performance in 2200 cases. Telemed J. 1999 Winter;5(4):323-37.PMID: 10908448 [PubMed - indexed for MEDLINE]

[21] Daniel C, García Rojo M, Bourquard K, Henin D, Schrader T, Della Mea V, Gilbertson J, Beckwith BA. Standards to support information systems integration in anatomic pathology. Arch Pathol Lab Med. 2009 Nov;133(11):1841-9.PMID: 19886721 [PubMed - indexed for MEDLINE]

[22] Dee FR. Virtual microscopy in pathology education. Hum Pathol. 2009 Aug;40(8):1112-21. Epub 2009 Jun 21.PMID: 19540551 [PubMed - indexed for MEDLINE]

[23] Dee FR, Meyerholz DK. Teaching medical pathology in the twenty-first century: virtual microscopy applications. J Vet Med Educ. 2007 Fall;34(4):431-6.PMID: 18287469 [PubMed - indexed for MEDLINE]

[24] Bruch LA, De Young BR, Kreiter CD, Haugen TH, Leaven TC, Dee FR. Competency assessment of residents in surgical pathology using virtual microscopy. Hum Pathol. 2009 Aug;40(8):1122-8. Epub 2009 Jun 24.PMID: 19552936 [PubMed - indexed for MEDLINE]

[25] Evans AJ, Chetty R, Clarke BA, Croul S, Ghazarian DM, Kiehl TR, Ordonez BP, Ilaalagan S, Asa SL. Primary frozen section diagnosis by robotic microscopy and virtual slide telepathology: the University Health Network experience. Semin Diagn Pathol. 2009 Nov;26(4):165-76.

[26] Horbinski C, Wiley CA. Comparison of telepathology systems in neuropathological intraoperative consultations. Neuropathology. 2009 Dec;29(6):655-63. Epub 2009 Apr 21.PMID: 19422534 [PubMed - in process]

[27] López AM, Graham AR, Barker GP, Richter LC, Krupinski EA, Lian F, Grasso LL, Miller A, Kreykes LN, Henderson JT, Bhattacharyya AK, Weinstein RS. Virtual slide telepathology enables an innovative telehealth rapid breast care clinic. Semin Diagn Pathol. 2009 Nov;26(4):177-86.PMID: 20069779 [PubMed]

[28] Dunn BE, Choi H, Recla DL, Kerr SE, Wagenman BL. Robotic surgical telepathology between the Iron Mountain and Milwaukee Department of Veterans Affairs Medical Centers: a twelve year experience. Semin Diagn Pathol. 2009 Nov;26(4):187-93.PMID: 20069780 [PubMed]

Differentiating Stained Tissue Structures Having Subtle Colorimetric Difference by Multispectral Image Enhancement

Pinky A. Bautista[1], Tokiya Abe[2], Masahiro Yamaguchi[2], Nagaaki Ohyama[2], John Gilbertson[1],Yukako Yagi[1]

[1]Harvard Medical School, [2]Tokyo Institute of Technology
email: pbautista@partners.org

***Abstract*— From a hematoxylin and eosin (H&E) stained tissue slide some of the eosin stained structures acquired inconspicuous staining patterns and to clearly differentiate them it requires the application of special stains. For example smooth muscle and collagen fibers, which could hardly be differentiated from an H&E stained slide, can be differentiated with the use of Masson's trichrome stain which distinctly gives the collagen fiber a different color from the smooth muscle. In this paper we utilized a 16-band multispectral imaging system to capture sample images of H&E stained tissue slides and applied a multispectral enhancement scheme to the images to delineate collagen fiber and smooth muscle. Results of our experiment showed that with multispectral imaging, especially with the application of multispectral enhancement, smooth muscle and collagen fiber can be differentiated. A comparison between the conventional RGB imaging and multispectral imaging to delineate tissue structures with subtle colorimetric difference was also performed. The results of the comparison showed the superior capability of using multispectral information to differentiate tissue structures which appear inconspicuous to the human.**

***Index Terms*—Multispectral, enhancement, pathology**

I. INTRODUCTION

Chemical staining is undertaken to improve the contrast of the original tissue. Tissue components can be generally categorized as acidophilic or basophilic and Hematoxylin and Eosin (H&E) dyes are popularly used to visualize tissue components according to this category; hematoxylin stains the acidic components of nuclei and cytoplasm while eosin stains the basic proteins in the cytoplasm and connective tissue (collagen, red blood cells, ect.). Nuclei are referred to as basophilic because its molecules bind to the basic hematoxylin dye pigment and the cytoplasm and connective tissues are also called acidophilic because they bind to the acidic eosin dye. The tissue areas that are stained with hematoxylin are impressed with a blue to black color while those that are stained with eosin appears red to pink. Although from an H&E stained tissue slide abnormalities that can be correlated to certain disease can be observed, pathologists still resort to special stains to qualify and quantify the specifics of the disease. For diseases related to the abnormality of the collagen fiber special stain such as Masson's trichrome (MT) is utilized to emphasize its presence and further assess the extent of its abnormality.

Collagen and smooth muscle are both stained with eosin dye and acquired similar staining pattern. Their difference could hardly be observed from an H&E stained slide since aside from sharing similar staining pattern they also share similarity in their morphology and structural pattern. Discrimination between collagen fiber and smooth muscle proves to be especially difficult. Hence the sensitivity of an imaging system is an important factor to derive salient information for the classification of these structures.

The potential of digital processing techniques to improve the quality of pathological images is already widely accepted where the intelligent used of digital algorithms for pathological image analysis to enhance the reproducibility of a diagnosis has been a subject of various researches [6-10]**.** Aside from the development of new algorithms some researchers focus on the application of multispectral imaging, which was originally designed to address space-based imaging problems, to improve the accuracy of image analyses results [1-5,11-13]. The main difference between the conventional RGB imaging system, which is commonly utilized to capture color images, lies in the bandwidth and the number of the color filters that are being used - multispectral imaging system employs N>3 narrowband filters in contrast to the conventional RGB imaging which utilizes three (3) broadband filters.

Due the sensitivity of the spectral filters in multispectral imaging systems salient image features, which are otherwise masked in an RGB image, can be captured. In this paper we will explore the capability of multispectral imaging system to differentiate H&E stained tissue structures which do not only share similar spectral characteristics but also structural. Visualization and differentiation of these structures will be done by enhancing the H&E stained multispectral images using the respective spectral transmittance of pre-identified tissue components, i.e. nucleus, cytoplasm, red blood cells (rbc), etc.. A comparison between multispectral imaging system and the conventional RGB imaging

system with respect to delineating tissue structures with inconspicuous spectral color difference will be undertaken as well.

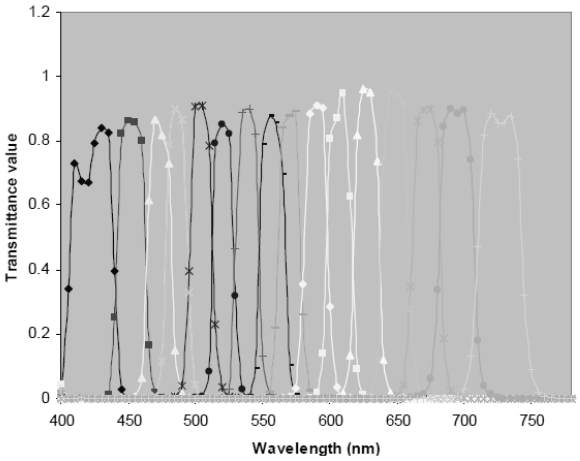

Fig. 1**.** The spectral sensitivity of the 16-band filter

II. MATERIALS AND METHODS

A. Multispectral image acquisition system

Tokyo Institute of Technology in collaboration with the Natural Vision project of Japan, developed a multispectral microscopic imaging system[14]. The imaging system utilizes 16 interference filters which are mounted on a rotating tablet; the spectral sensitivities of these filters are shown in fig.1. The system houses a CCD camera which enables the user to capture a 2Kx2k pixels image of 16-bit per pixel at different objective magnifications, e.g. 10x, 20x, 40x. The microscope is connected to a PC which is equipped with software that allows control of the microscope. With this software user can interactively select areas of interest and view their respective spectral transmittance as well. The set-up of this multispectral microscopic imaging system is shown in fig. 2.

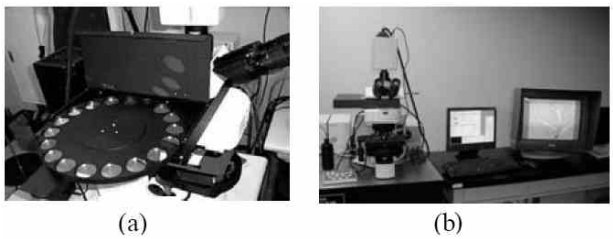

Fig. 2 The 16-band microscopic multispectral system. (a) the 16-band rotating filter tablet; (b) the set of the multispectral camera wherein the microscope is connected

B. Tissue images

From the H&E and Masson's trichrome (MT) stained images of a heart tissue we captured three pairs of multispectral images. These images contain collagen fiber, and other tissue structures whose difference from collagen fiber is not easily discernable when viewed from the H&E stained images, however they are well differentiated from their MT-stained images counterpart. The H&E and MT stained tissue slides come from the serial section of a heart tissue so that there is correlation in the tissue make-up between H&E and MT-stained images. Although we used images of heart tissue, the enhancement method that is described in the succeeding section can also be applied to tissues of different types. The initial choice of a heart tissue was motivated by the clear illustration of smooth muscle and collagen muscle.

C. Spectral transmittance calculation

The captured multispectral image is composed of 16 2kx2k grey level images that represent the light sensitivity of the filter at different wavelengths. To calculate for the spectral transmittance of each image pixel, two types of images are captured, namely the tissue image and the glass image. Denoting the intensity value of the pixel at location *x,y* for the specimen and glass images as i and i_0 respectively, the spectral transmittance of such pixel can be calculated as follows:

$$t = i / i_0 \qquad (1)$$

where t , i , i_0 are column vectors of dimension 16x1.

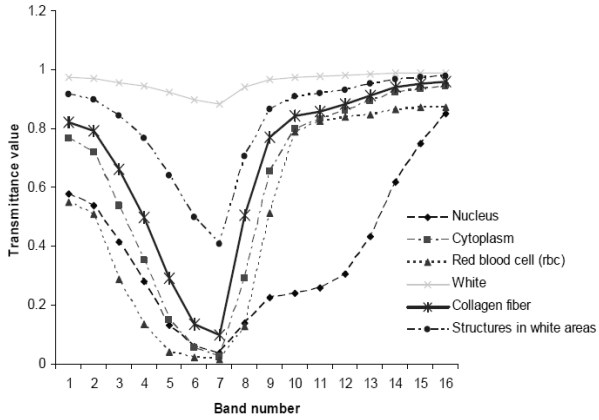

Fig.3 The average spectral transmittance of the different tissue components that were identified from the training image.

D. Spectral transmittance data set

The tissue components that have different dye affinities such us the cytoplasm and nucleus are expected to demonstrate distinct spectral transmittance characteristics. From one of the images that were captured we identified 6 tissue components, i.e nucleus, cytoplasm, red blood cell (rbc), white, collagen fiber and structures in white areas. Of these six tissue components only nucleus shows strong affinity to hematoxylin dye and the rest, except the white area, show affinity to eosin dye. We picked 200 representative samples for each tissue component. Figure 3 illustrates the average spectral transmittance of these tissue components. Although from these spectra we can observe distinctions between the eosin stained tissue components spectra, there are areas in the H&E stained image that are closely similar to collagen fiber but are not necessarily collagen fiber when we probe their staining patterns in the equivalent MT stained image. We will show in the following sections that these areas can be delineated once multispectral enhancement is performed.

E. Multispectral enhancement

An enhancement scheme for multispectral skin image has been proposed by Mitsui et.al [15] to differentiate abnormal skin areas from normal areas. In this paper we extend such method to accommodate the inherent characteristic of histopathology images wherein not only two classes of tissue components exist but multiple classes.

The enhancement method utilizes the spectral difference between the image pixel's original spectral transmittance and its estimated value using some number of PC vectors. Let us suppose that the original spectral transmittance of a tissue component is denoted by t and the estimated spectral transmittance estimated by M principal component (PC) vectors is denoted by $\tilde{t}$. The original transmittance can be altered by the following:

$$t_e = t + W\left(t - \tilde{t}\right) \qquad (2)$$

Where t_e is a column vector of dimension Nx1 that represents altered transmittance equivalent of the original transmittance t ; W is an NxN, i.e. N=16, weighting matrix whose entries serve as the modulating factors to the difference between the original and estimated spectral transmittance at particular bands. While in [15] only the diagonal entries of the matrix W are given non-zero values in the current work we utilized the off diagonal entries as well. The hue of the enhanced image is governed by the column of the W and the direction of the entries. On the other hand, the color intensity is governed by the magnitude of the entries.

F. Spectral estimation by PCA

The spectral transmittance of an image pixel can be estimated using *a priori* analysis in which case the widely used technique is principal component analysis (PCA). In this technique a set of spectral transmittance R_{NxM} ,, i.e. N is the spectral dimension and M is the number of spectral samples, is used to derive the N PC vectors. Using only $M<N$ PC vectors the original transmittance can be reconstructed within certain degree of error. For the purpose of the multispectral enhancement the transmittance data set is made to consist of the transmittance samples of all the identified tissue components except for the transmittance spectra of the tissue components which are desired to be enhanced and differentiated and in our case this is the collagen fiber. From the application of the principal component analysis (PCA) on the spectral transmittance data set we could derive the N PC vectors which can be used to reconstruct the original spectral transmittance t of an image pixel. We can reconstruct the spectral transmittance using the PC vectors by the following:

$$t = \sum_{i}^{M} \alpha_i v_i + \bar{t} \qquad (3)$$

where v_i is the *ith* PC vector and α_i is its corresponding PC coefficient; and $\bar{t}$ is the average transmittance calculated from R_{NxM} [15]. In PCA the low order PC vectors or PC bases account for as much of the data variability and the succeeding bases account for the remaining variability. Using only $M<N$ low order PC bases we can explicitly express eqn.3 as follows:

$$\tilde{t} = \sum_{i}^{M} \alpha_i v_i + \bar{t} \qquad (3a)$$

We used the result of eqn. 3a to generate the enhanced transmittance spectra in eqn.2. The resulting enhanced 16-band spectral transmittance is then converted to its RGB equivalent values to produce an image perceptible to the human eyes.

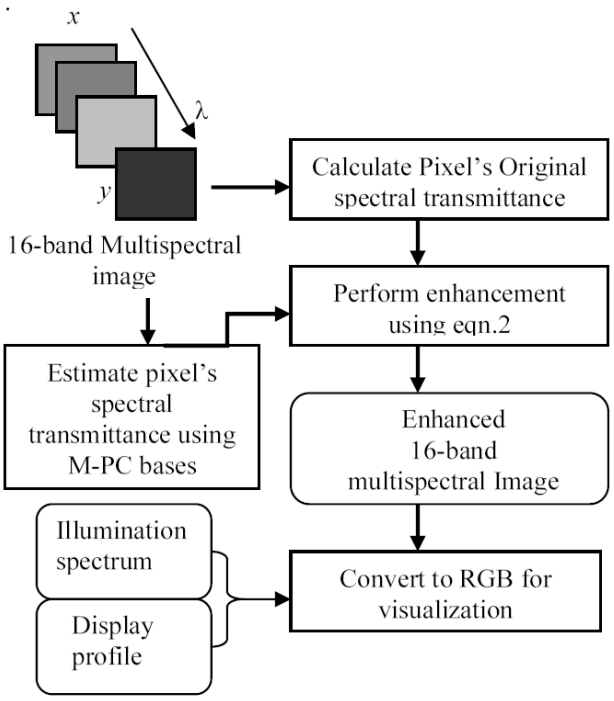

Fig.4 Multispectral enhancement method to visualize tissue structures which exhibit close colorimetric attributes.

III. RESULTS AND DISCUSSIONS

Figure 4 outlines the processes that were done to visualize collagen fiber from the rest of the eosin stained tissue structures from the H&E stained multispectral multispectral pixel is calculated and then modified by applying eqn. 2. The tissue components which are affected by the transmittance modification are mainly those which were not represented in the data matrix R_{NxM} and these are the tissue components which are desired to be enhanced and differentiated, i.e. collagen fiber and smooth muscle. The 16-band enhanced multispectral image is converted to RGB format for visualization.

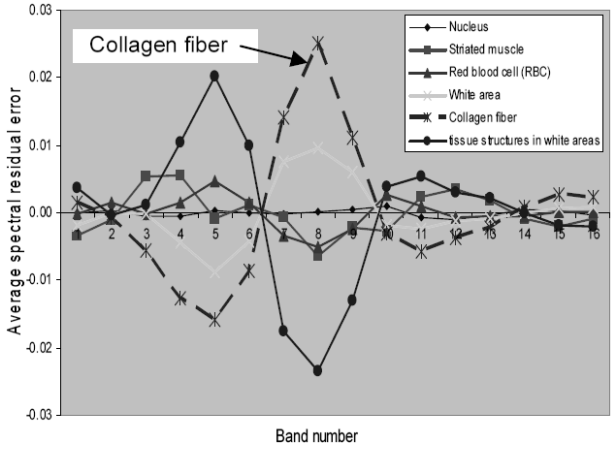

(a)

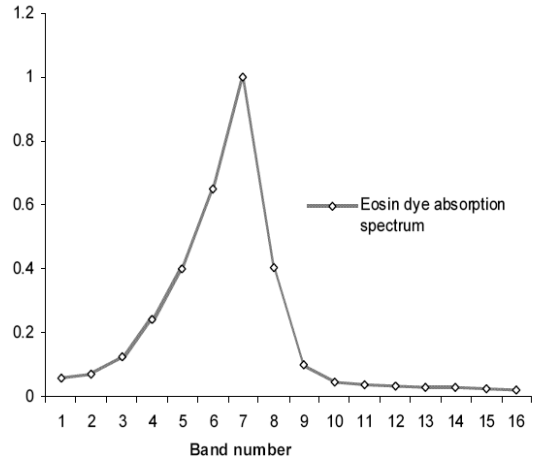

(b)

Fig.5 (a) Average spectral error of the different tissue components using 5 PC vectors. This error curve shows similar trendency when compared to the absorption spectrum of eosin dye in (b). Moreover it is to be noted that collagen fiber exhibits distinct peak particularly at band 8. (b) The absorption spectrum of eosin dye showing that it has a peak at band 7.

A. Effective number of PC vectors

We defined the spectral error as the difference between the original transmittance t and the estimated transmittance $\tilde{t}$:

$$e = t - \tilde{t} \quad , \qquad (4)$$

where e is a 16x1 column vector. We determined the appropriate number of PC vectors with which the spectral error of the tissue components that are not represented in the training data set R_{NxM} . acquired distinct peaks at some specific wavelengths while those tissue components whose transmittance spectra are used in R_{NxM} are relatively low. We examined the spectral errors of the different tissue components whose spectral transmittance configurations are illustrated in fig.5a for different number of PC vectors and we found that with 5 PC vectors distinct spectral error pattern for collagen fiber can be observed. It should be noted however that the effective number of PC vectors is affected by the classes of spectral samples used in the training data set.

B. Spectral error

The average spectral errors of the different tissue components that we have identified in this experiment using 5 PC vectors are plotted in fig.5a. We can observe that collagen fiber exhibit distinct peaks at certain band numbers (or wavelengths). The collagen fibers are stained pink with eosin dye and a close comparison between the characteristic curve of the eosin absorption spectrum in fig.5b and the spectral error of collagen fiber reveals a similarity. Both the eosin spectrum and spectral error of the collagen exhibit peaks at the mid spectral range. However while the eosin spectrum peaks at band 7, the spectral residual error exhibit its peak at band 8. It can be thought that the spectral color difference between eosin stained tissue structures can be due to their differing staining reaction to the dye, and that this reaction causes a shift in the eosin spectrum.

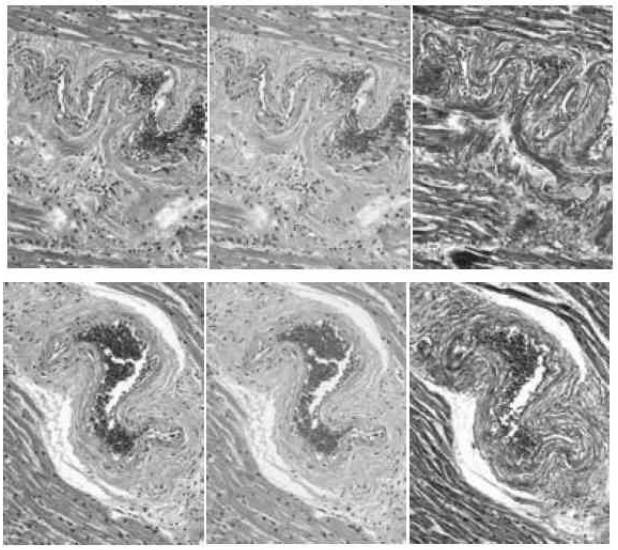

(a) (b) (c)

Fig.6 The H&E stained images and their enhanced versions, together with their corresponding Masson's trichrome stained impressions. (a) Original H&E stained images; (b) result of the multispectral enhancement; (c) Corresponding Masson's trichrome(MT) stained impression of the given H&E stained images. It is to be noted that the MT and H&E stained tissue slides are of serial sections so that they share similarities in their structural make-up.

C. Multispectral enhancement

The mathematical operation that governs the multispectral enhancement process is illustrated by eqn. 2. The color visualization of the collagen fiber depends on which columns of the weighting matrix W are activated and the magnitude and polarity of the entries. The determination on which entries of the matrix W should be given non-zero values and whether it should be negative or positive can be referred to the spectral of the collagen fiber. For example we can observe that at band 9 the error of the collagen fiber peaks then we can assign non-positive values for the entry corresponding to W(9,9) of the matrix W. To give more variation in the color of the enhanced image instead of concentrating on

a single entry of the matrix as what was done in [15] not only a single element of the matrix was assigned with nonzero values. In the current experiment non-zero values were assigned to columns 5-9 of the weighting matrix W. Result of the multispectral enhancement using 5 PC vectors for the heart images are shown in fig.6. The images on the first column are the original H&E stained images, and the middle column illustrates the enhanced version of these images. The enhanced images are compared to the MT-stained equivalent of the original H&E stained images, which are located at the rightmost column. We can observe that there is a strong correspondence between the emphasized areas in the enhanced images to the areas which are stained blue in the MT-stained images.

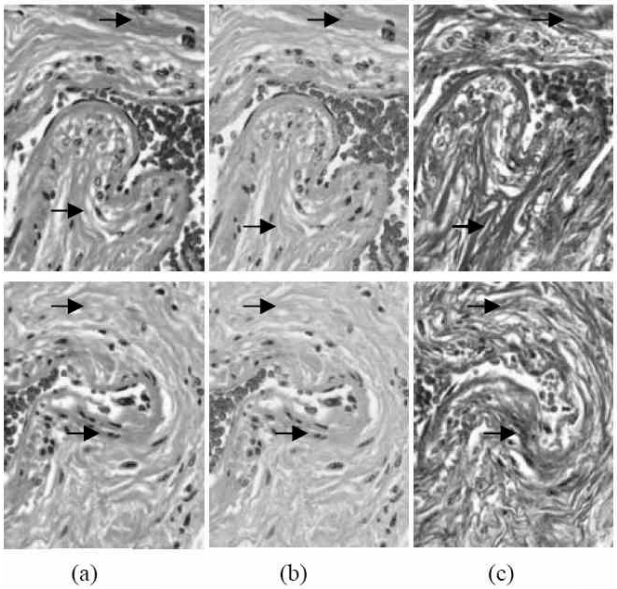

Fig.7 An illustration of an image area whereby similarly stained tissue structures show differing spectral response as illustrated by their varying color in the enhanced version of the H&E stained images. These axb pixels images were cropped from the original 2kx2k pixels image. (a) Original H&E stained; (b) Enhanced version of the H&E stained images; (c) Equivalent Masson's trichrome stained images of the H&E stained images, which serve as reference for the enhanced images.

To further examine how multispectral imaging with our multispectral enhancement scheme fare with respect to delineating tissue structures that are inconspicuously similar both in their morphological or spectral color features, we cropped one of the areas that contain these structures and view them at higher digital magnification. We can see from fig. 7 that the areas which are indicated by arrows could hardly be differentiated from collagen fiber in the H&E stained images but are now differentiated in the digitally enhanced images.

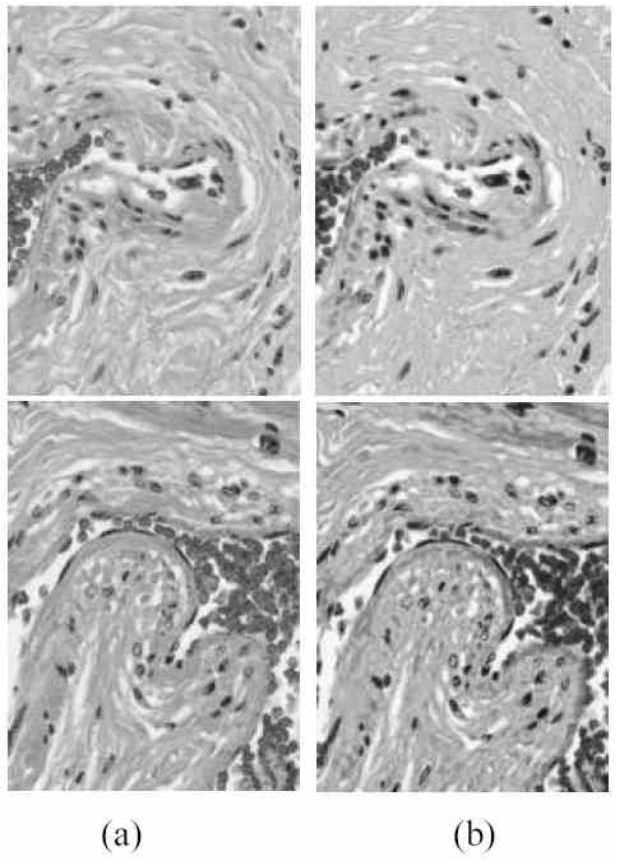

Fig.8 A comparison between the enhancement results using RGB and multispectral information, specifically in image areas where tissue structures acquired similar staining pattern. (a) Enhancement results using RGB information; (b) Enhancement results using multispectral information;

D. RGB and multispectral imaging

The microscopic RGB imaging systems used in most laboratories employ 3 wideband filters that have spectral sensitivities in the red, green and blue channels. In contrary a microscopic multispectral imaging system employs N>3 narrowband filters. To compare how RGB and multispectral imaging fares in differentiating collagen fiber from the rest of eosin stained tissue structures we also tried to enhance the equivalent RGB image of the multispectral H&E stained images. For the RGB enhancement we used one of the functions in the PHOTOSHOP imaging software to change the hue of the supposed collagen areas. The RGB image of the H&E stained image was imported into Photoshop and a point located in the collagen fiber area was selected as reference for changing the color of the rest of the collagen fiber areas. Figure 8 shows the enhancement results using RGB and multispectral information. We can see that while enhancement with multispectral information results to clear differentiation between structures that are apparently similar when viewed from an H&E stained image, but show distinctive features, i.e. spectral color when stained with special stain such as Masson's trichrome (MT), enhancement with RGB failed to provide distinction between these areas. From these results it can be said that multispectral imaging can

capture salient spectral features that enabled us to differentiate these areas.

Spectral color of stained tissue structures may reflect its reaction to a dye and that even a small change in the respective spectral transmittance of tissue structures may provide significant impact to their differentiation. The plot in fig.9a demonstrates the 16-band spectral transmittance of two sample points selected from the area occupied by collagen fiber1 and that of the tissue structure which appear to be similarly stained with it, which we refer as collagen fiber2; we can see from this plot that there is a small difference between these structures. A close observation of the plots reveals a shift at band 8, i.e. collagen fiber1 becomes more positive than collagen fiber2. This correlates to the spectral error peak at band 8 which is illustrated in fig.5a. This small difference in spectral transmittance may not be necessarily evident from the RGB spectra shown in fig. 9b. The RGB spectra were simulated by taking the average transmittance value of bands 1- 5 for blue channel, bands 6-10 for green channel, and bands 11-16 for red channel. We can note that the RGB spectral plot for both tissue structures coincides, which implies that differentiation between these two structures using RGB information is difficult.

IV. CONCLUSIONS

Differentiation between tissue structures sharing close colorimetric attributes has its impact not only for H&E stained slides but even for immuno stained slides where reactions are labeled either positive or negative depending on the intensity of the staining. We have shown in this paper that these minute differences can be exploited for their better visualization and differentiation using multispectral information. Although the conventional (broadband) RGB imaging is helpful for observing the general morphology of the tissue components, but for the delineation of structures, which normally requires the use of special stain, the inherent information of an RGB image is not sufficient enough.

Utilization of multispectral imaging to histopathological image analysis especially for the visualization of tissue structures which are not emphasize by the staining dyes is not fully addressed yet. In this work we have initially investigated the capability of multispectral imaging to differentiate tissue structures which have minute colorimetric difference. We have also shown its advantage over the conventional RGB imaging in visualizing and differentiating tissue structures which exhibit similarities both in their morphology and spectral color features. Utilization of multispectral imaging with the enhancement methodology presented herein is valuable particularly in the absence of special stain and visualization of specific tissue structures which is not necessarily highlighted in the current stained slide is called for to confirm the initial diagnosis. Digitally enhancing tissue images can also be very useful for telepathology whereby pathologists confer their respective diagnosis through the internet.

A thorough understanding on the driving force behind the spectral differences between similarly stained tissue structures can be very valuable in developing algorithms that can be ultimately applied for clinical use. Thus, part of our next work would be to investigate this particular phenomenon in detail. Other tissue types would also be considered to validate further the results presented herein.

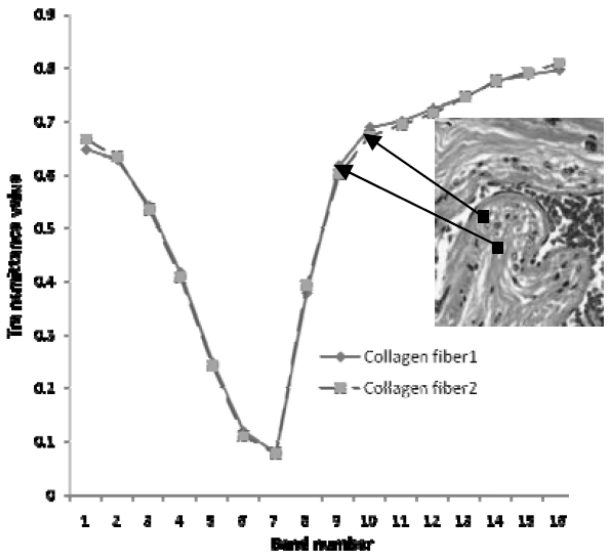

(a)

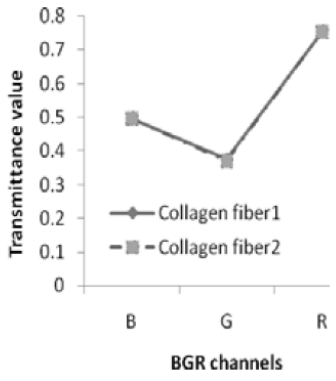

(b)

Fig. 9 Plots showing the spectral transmittance of two sample points extracted from image areas which have inconspicuous staining patterns. (a) 16-band spectral transmittance; (b) simulated RGB (or 3-band) spectral transmittance.

REFERENCES

[1] Lisa, L., Patricia A. Medvick, Harlan P. Foote, and James C. Solinsky: Multispectral/ Hyperspectral Image Enhancement for Biological Cell Analysis. Cytometry 2006, Part A 69A: 897-903

[2] Barber, P.R. Vojnovic,G. Atkin,et al: Applications of cost-effective spectral imaging microscopy in cancer research. J.Phys.D: Appl.Phys. 2003, 36: 1729

[3] Levenson, R. : Spectral Imaging Perspective on Cytomics. Cytometry Part A 69A, 2006: 592-600

[4] Guo, N. Zeng, L. and Wu, Q. : A Method based on multispectral imaging technique for White Blood Cell segmentation. Computers in Biology and Medicine, 2007 (37): 70-76.

[5]Liu,Y., Zhao, T. and Zhang, J.: Learning Multispectral texture

Features for Cervical Cancer Detection: Proceedings International Symposium on Biomedical Imaging:Macro to nano, 2002: 169-172.
[6] Petushi S., Garcia F. U., Haber ,M. M. et. al: Large-scale computations on histology images reveal grade-differentiating parameters for breast cancer. BMC Medical Imaging, 2006, 6(14)
[7] Doyle, S., Hwang, M., Shah, K., et al: Automated Grading Of Prostate Cancer Using Architectural and Textural Image Features. Proc. ISBI, 2007: 1284-1287
[8] Karacali, B. and Torezen, A.: Automated detection of regions of interest for tissue microarray experiments: an image texture analysis.BMC Medical Imaging, 2007,7(2)
[9] Masseroli, M., Caballero, T. , et.al: Automatic quantification of liver fibrosis: design and validation of new image analysis method: comparison and semi-quantitative indexes of fibrosis. J. of Hepatology, 2000, (32): 453-464.
[10] Munzenmayer, C., Paulus, D. and Wittenburg, T.: A spectral Color Correction Framework for Medical Applications. IEEE Trans. On Biomedical Engg. 2006, 53(2): 254-265
[11] Yamaguchi, M. : Medical Application of a Color Reproduction System with a Multispectral Camera. Digital Color Imaging in Biomedicine, 2001: 33-38
[12] Levenson, R.M., Cronin, P. J. and Harvey,N.R. : Spectral Imaging and Biomedicine: New Devices, New Approaches. Proc. IEEE 31st Applied Imagery Pattern Recognition Workshop, 2002
[13] F. Keiko M. Yamaguchi, N. Ohyama & K. Mukai. Development of support system for pathology using spectral transmittance- the quantification method of stain conditions. *Proc SPIE Medical Imaging Proc*., 2002, 4684: 1516-1523
[14] Fukuda, H., Ohyama, N.,et al, APIII, Pittsburgh, PA, 2002, http://apiii.upmc.edu.html
[15] Mitsui, M., Murakami,Y.,et al: Color Enhancement in Multispectral Image Using the Karhunen-Loeve Transform: Optical Review 2005,12(2): 60-75

AI (artificial intelligence): from Image Analysis via Automated Diagnosis to Grid Technology

Klaus Kayser[1], Jürgen Görtler[2], Aleksandar Bogovac[1], Milica Bogovac[1], Gian Kayser[3]

[1]IUCC-TPCC, Institute of Pathology, Charite, Berlin, Germany; [2]IBM Deep Computing, Amsterdam, The Netherlands; [3]Institute of Pathology, University of Freiburg, Freiburg, Germany

Abstract—**The digitalization of a complete glass slide opens new doors in nearly all fields of tissue – based diagnosis (diagnostic pathology). A virtual slide offers access to applying a set of algorithms which can support the diagnostic pathologist's daily work. Good image quality is essential to detecting visual information that can be translated into a final diagnosis. Parameters of image quality include in addition to classic features object size in relation to the image size, distribution and maximum height of gray values as well as homogeneity of illumination. Derived parameters are number and distances of potential segmentation thresholds and the features of the corresponding gradient image. A transformed standardized (reference) image can be used for standardized measurements. Image quality measurements and derived image standardization are embedded in the automated immunohistochemical measurement system EAMUS™ accessible via the internet (www.diagnomX.eu). Measurement of object features, the derived structure, and features based upon pixel gray values and distribution (texture) can serve for an automated diagnosis algorithm. Texture features are computed using an auto regression method derived from time series analysis, object features after active segmentation methods with added extern knowledge and stratified sampling, structure features by application of Voronoi's neighborhood definition (tessellation) and syntactic structure analysis. Multivariate discriminate analysis with inbuilt feedback mechanism required a training set of 10 cases per diagnosis only. The accuracy of final classification measured 96 – 100 % for crude tumor classification of various organs including breast, colon, lung, pleura, and stomach. Adding tools of automated detection of area of interest and common communication standards serving for accurate tumor screening in virtual slides build the basis and the capability to embed a developed system into a Grid environment. This Grid environment enables a collaborative working approach among participating pathologists.**

Index terms—**Virtual slide, image quality, automated diagnosis, Grid technology**

I. Introduction

Tissue – based diagnosis or diagnostic pathology derives a disease classification called diagnosis from specifically altered appearance of biological meaningful units in combination with clinical data [1]. Biological meaningful units are circumscribed visual objects with specific functions that can be visualized by various techniques such as conventional stains (H&E), immunohistochemical methods (specific antibodies (or carbohydrate ligands) with attached chromogens binding to cells or cell compartments), enzyme repetitive functions (polymerase chain reaction, in situ hybridization) or other detection methods (electron microscopy, spectral analysis, etc.). Size and gray value associated features of these objects as well as the spatial distribution of the objects are often closely associated with a certain disease; thus they serve for accurate disease recognition or diagnosis such as cancer, tuberculosis, parasites, or virus infections [2]. These units often can be transformed by symmetry transformations. The result of such a transformation can serve as a new unit visible at different (lower) magnification. The concept is called order of structures, and has been described in detail in [3-5]. It requires a neighborhood condition (most frequently used are Voronoi's tessellation and O'Callaghan's neighborhood condition). Practical calculations have been performed by graph theory applications [6].

The concept of "orders of structures" serves as theoretical basis to implementing the only crude described "diagnosis evaluation" by a diagnostic pathologist into computerized algorithms. One aim of digital pathology is to assist the pathologist in pre-screening and diagnosis-likelihood information in order to pursue the increasing work load and maintain or even improve the diagnostic quality.

The details of the concept and practical experiences are described herein. In addition, we will give perspectives of the possible development direction of this technique.

II. Basic Diagnosis Algorithm

According to the present understanding of visual tissue – based diagnosis the general diagnostic algorithm is a function of image texture and contemporary of the recognition of biological objects (segmented units) [7]. In other words, diagnosis = f (texture, magnification (objective), object, structure). The terms texture, object, structure have to be defined in an unequivocally manner.

The definition of texture is usually quite crude [8] classified textures according to the items coarseness,

contrast, directionality, line-likeness, regularity, and roughness. These terms are difficult to implements in a digital system. We, therefore, use a different definition, first described by Voss [9]. It is derived from time series analysis and uses a pixel – based recursion formula. It results in a reproductive algorithm and is a useful method to be implemented in a diagnostic algorithm. No segmentation of the image is required as well as no external information, i.e., predefined parameters to include/exclude results which do not fulfill certain limitations, for example in size, gray value distribution, boundaries, etc.).

On the other side, objects have to be detected within the image. They are dependent upon external information and usually require a segmentation algorithm. We prefer to basically divide an image into an object space and a background space prior to the actual segmentation. Virtual slides are commonly composed of quite large areas that do not contain any tissue, and, thus, cannot contain objects [1]. A simple segmentation threshold is sufficient for the identification of potentially object containing areas (object space). Within this space objects have to be identified, and to be distinguished from artifacts [1]. Parameters of potentially detected objects include size, gray value distribution within the detected unit, identification of its boundary, and derived features (moment, form factor, entropy, etc.). External information which can be adjusted to the image magnification (i.e. absolute pixel size) is essential.

The identification of objects automatically includes the location of the gravity centers, which then serve for the construction of structures [2]. Voronoi's and the derived Dirichlet's tessellation are widely used, less common applied is O'Callaghan's neighborhood condition [10, 11]. The graph theory provides appropriate tools to further apply image transformations in order to detect symmetries or repetitive arrangement of objects such as "rings", "lines", "stars", etc. Their centers of gravity can be considered as "new objects" located within a different magnification space [3]. It can reallocate a new (independent) set of features to be applied in the diagnostic algorithm [1]. A survey of the diagnostic algorithm is demonstrated in [Figure 1].

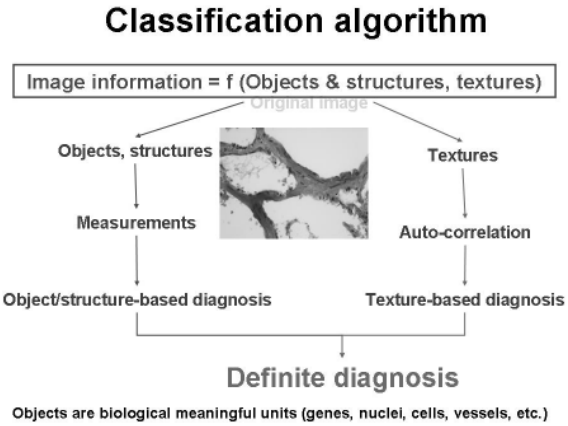

Figure 1: Scheme of automated classification algorithm to be applied in tissue based diagnosis.

III. Area Of Interest

Any diagnostic algorithm to be applied in tissue – based diagnosis depends upon the selected area of interest [6, 12, 13]. The area of interest is a compartment of the virtual slide that contains the visual information most significantly associated with the tissue – based diagnosis of the highest clinical importance [2]. Examples are cancer cells in a body fluid that contains numerous inflammatory cells, or a small metastasis in otherwise normal or only reactive inflammatory altered liver or lung tissue. The detection of these diagnosis significant areas is basically associated with a sampling procedure [14] The human performance prefers a screening at "low magnification", followed by a precise identification of objects (nuclei, cells). A computerized method might try to first identify the included objects and afterwards derive the most instructive areas dependent upon the detected objects [14]. This algorithm would require an analysis of the complete virtual slide at high or at least moderate magnification, which is certainly less effective compared to screen at low magnification, and identify objects at instructive areas at high magnification.

The application of texture analysis seems a promising method to search for significant areas of interest [14]. A method described by Belhomme and Coifman uses spectral analysis techniques to identify areas of interest [15] [16]. Most virtual slide scanners are provided with a threshold – adapted algorithm to separate "tissue containing areas" from the background [17]. The technique saves image storing space and provides faster access to the virtual slide.

When dividing the virtual slide in attaching compartments at low magnification, texture changes at the boundaries and in association with the boundaries can serve for separating normal from altered tissue [18]. The sensitivity threshold is as low as 5 % of the compartment's area, i.e. tumor growth can be detected at the level of micrometastases [18]. The algorithm can be applied at one-color images obtained by principal component transformation as well as on images presented in various color spaces (rgb, his, etc.) [19]

The described methods to detect areas of interest in a virtual slide do not require external information [1, 15, 16]. Thus, they are not associated with the knowledge or suggestion of a diagnosis, and can be applied in general.

IV. Image Quality

The better the image quality the easier, more sensitive, and specific are the diagnosis algorithm in general. A given image has to be standardized if it does not fulfill certain quality measures. This simple statement is known to all diagnostic pathologists who usually require slides stained in the laboratory they are used to work with. How to standardize histopathology images?

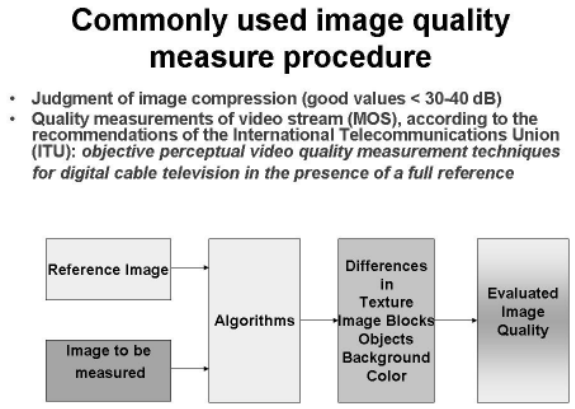

Figure 2: Commonly used measure of image quality: the actual image is compared to a "reference" image.

All measurements of image quality use a comparative method [20] and compare the actual image with a reference image as shown in [Figure 2]. Distances between the two images are a measure of image quality. In addition to subjective measures there are basically two different features of image quality: 1) those affecting the complete image independently from its information content, and 2) those related to information content (objects, structures). The first features include illumination, total gray value distribution, and gray value range. They can be optimized by appropriate transformations, i.e., shading correction, gray value shift and expansion (compression) in relation to the pixel coordinates [7]. The second features are related to pre-defined algorithms that are used to detect and identify objects (and their associated structures). We suggest the following procedures. Any object identification requires at least segmentation, and any segmentation method definition of at least one (not necessarily coordinates independent) gray value threshold. The more distinct and the broader the gray value differences between the detected thresholds the easier the segmentation procedure can be applied [18]. An example is demonstrated in [Figure 3]. The algorithm can be applied to either the principle component transformed image or to any color space [7]. The transformation of an image into the hsi (hue, saturation, intensity) color space permits an easy recognition of images with good quality, as demonstrated in [Figure 4].

The image obtained by the quality correction transformations serves as reference image and is subject for automated image measurements [7]. The measured differences between the actual and reference image can be stored in a series, and permits a consecutive viewing of image quality development.

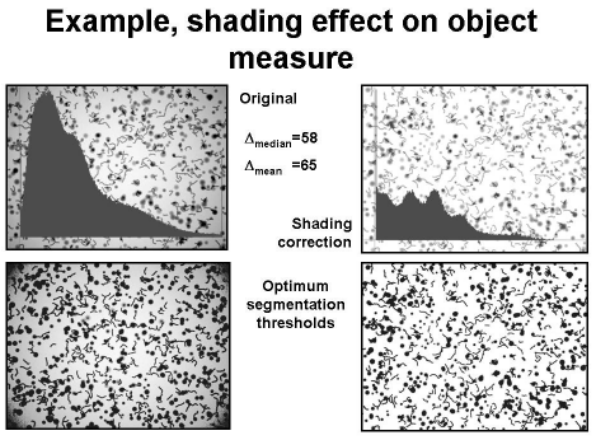

Figure 3: Example of influence of image quality on segmentation thresholds and segmented objects (shading correction provides improved segmentation thresholds.

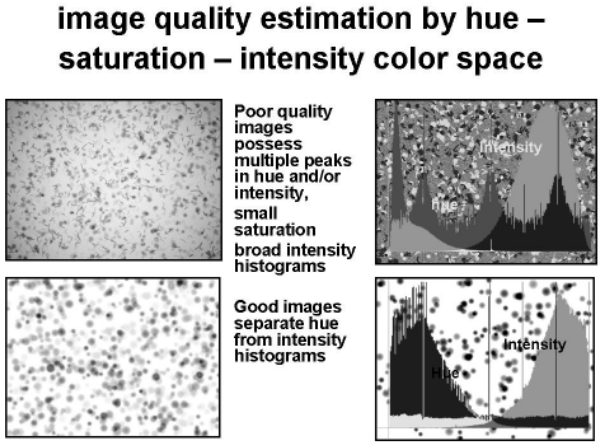

Figure 4: Example of image quality measure in his space: images of good quality display a clear separation of hue – intensity spaces.

V. Automated Measurements

Having discussed how to construct a diagnostic algorithm, how to evaluate image quality, and how to provide a standardized image, we have the tools to implement an automated image measurement system [21]. Such a system has to identify objects, and thus requires some external information to be provided by the user. The essential minimum information includes:

1. Which kind of information should be evaluated (i.e., which measurements should be performed)?
2. What are the expected features of the objects (this information reflects to the image magnification)?
3. Is there a color space reference of objects (this information corresponds to the staining procedure or visualization dye in case of immunohistochemistry)?
4. Where and how should the results be provided (this information corresponds to format of provided results (for example <.txt> or <.csv>, and the user's email)?

Such a system can be installed in the internet by appropriate programs (for example written in Java or

php language). The EAMUS™ system is, to our knowledge, the first implementation, which is available in the internet via www.diagnomX.eu. It has been designed for immunohistochemistry measurements including fluorescence stains and DNA fractions analysis (Comet measurements). Its principle structure is shown in [Figure 5], its implemented measurements comprise nuclear, membrane, vascular, and area estimates. More than 30 users are registered and use this system in either measuring individual cases or image series (for example tissue micro arrays (TMAs)).

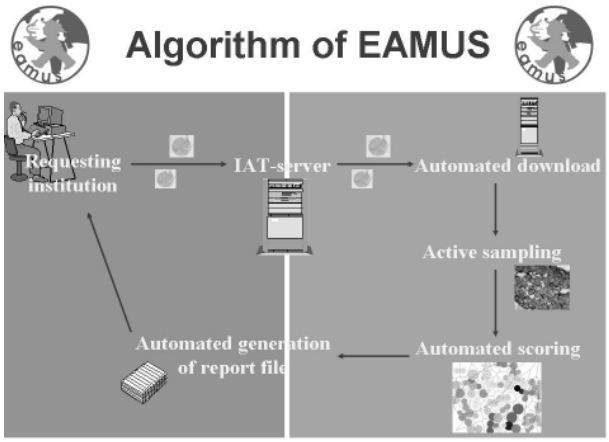

Figure 5: General scheme of the Internet embedded electronic automated measurement user system (EAMUS™; www.diagnomX.eu

VI. Automated Diagnosis

Automated measurements of texture, objects and image structure are a prerequisite to automatically create a tissue based diagnosis [7]. In addition, a classification system has to be provided which groups the evaluated data into the corresponding class (diagnosis) [22]. The external information required for automated object identification can be combined with the final classification set, especially if virtual slides are evaluated. If we want to distinguish between normal – inflammatory – tumorous lung tissue a hierarchic sequence of classification boxes seems to be appropriate. These boxes are usually predefined by external features, and usually correspond to a certain organ [18]. They can, however, also be automatically detected in a more complex system that contains corresponding feedback mechanisms [2].

Attempts to derive diagnoses from measured object features range back to the nearly forgotten roots of tissue – based diagnostics, i.e., the quite sophisticated technology of stereology that had been developed in the sixties of last century [23]. Stereology takes into account the "real" object size in our three dimensional space, its projection to a two dimensional plane, and correction of artifacts. Numerous articles have been published demonstrating a close relationship between cell (nuclear) features and various diseases since the middle of the last century [24]. However, none of these approaches have been introduced into routine diagnostic pathology, and consecutively, most pathologists are convinced that attempts of image quantification are not appropriate to be applied for diagnostic purposes.

Maybe one of the root causes for such positions was also the challenge of evaluating of a huge matrix, which could be only done rudimentary without the supporting tools and depended on the experience of the pathologist.

Why are we optimistic that we have reached a more promising level of this vision?

The idea of contemporary measurements of texture and object-related features has been derived from previous data that have given satisfactory relations between the measurement results and the underlying diagnoses, see for example [4]. Whereas most (if not all) of these attempts in detail describe the obtained features and their measures, see for example [25], recent approaches do not focus on these features [18]]To the contrast, the are flexibly embedded in statistical correlation procedures that allow to defining new data sets and outcome ranges if the input data smoothly change (for example associated with the stage of the disease or the age of the patients) [18]. Thus, the data input source is a flexible and self adjusting system, and not a fixed data set. It should work, in principle, for all diseases or tissue based diagnoses [18].

An open and standardized access as well as a standardized and flexible output is the second difference. Such a system could run in the background and search for data that allow a substantial diagnostic assistance of the actual case [17]. Internet embedding of a standardized portal with direct connection to the specific measurement programs is on its way and will provide the necessary experience and information for further development of automated diagnostic systems [2].

VII. Grid Technology

The proposed tools have to be made available in a technical environment to enable the catalogues growing by any pathologist to contribute, and databases and to allow pathologists to make the best use of it. Grid technology provides the architecture for this type of infrastructures.

In addition to the discussed information technology structures that basically include multiple open accesses and one or only a few fixed computational nodes one could think about the distribution of all necessary elements in a system that primarily is constructed upon platforms [17, 26]. Such a system is called a Grid. Naturally, these platforms (or nodes) require strict standards in order to communicate in between. The standards are provided by the Internet. Thus, a Grid is an Internet embedded network consisting of a broad variety of connected nodes. These nodes can be compared to servers and assure a platform of communication standards, which permit the users to concentrate solely on their individual tasks. The function of a Grid is a network computing, and can be considered to be a derivative of the development and maturation of the Internet The idea is to distribute high power computations to several computers that will work

contemporarily on the same problem, for example in high energy physics, molecular modeling, or astrophysics [27, 28]. Network computing is also called metacomputing, scalable computing, global computing, or Internet computing. Grids can be applied for a broad variety of tasks, called services. These include computational services, data services, application services, information services, or knowledge services [17, 19]. All of these quite different services is in common that they include end users or clients, distribution and control nodes, and servers, anyone able to perform the requested tasks. A management software layer (Middleware) ensures the computer–based collaborative environment which also requires computation nodes, so – called brokers. A Grid sourced broker administers the workload, potential problems, discovers free resources, and controls the processing of the end user tasks. The clients are informed and have access by a presentation tier, which then standardizes the tasks and handles them to the internal executive network (service tier). The whole network is monitored by the resource tier that controls the workload of the computational nodes, the dynamic status and activity of the network [17, 19].

A tissue - based diagnostic Grid has not been developed until now. However, this kind of tool support for pathologists can offer significant advantages once the principle diagnostic algorithms have fully been developed and tested:

1. A pathologist working in a virtual microscopy environment could be significantly assisted by such a Grid in terms of image quality evaluation prior to the diagnostic procedure, pre-selection of most likely diagnoses, presentation of most informative slide areas, and selection of additional stains and laboratory procedures mandatory for a detailed final diagnosis.
2. Automated diagnosis assistance procedures could be implemented in pathology institutions specialized for different technical or diagnostic experiences. These include cytological, molecular genetic or biological methods, image analysis methods, databank handling, organ associated diagnostic pathology, and statistical analysis (neural networks, flexible and adjustable multivariate analysis, etc.).
3. Diagnosis quality evaluation could be performed on an automated, inter- and intra-observer independent level provided by automated image feature extraction and adjusted to the individual institutional collectives.
4. Data of specific interest such as rare diseases, endemic features, or survival could be analyzed in a joint manner provided by the implemented data, tasks, and performance standards.
5. Unknown diseases or unclassifiable results can be separated and submitted to specific diagnosis boards for further investigations.
5. Unknown diseases or unclassifiable results can be separated and submitted to specific diagnosis boards for further investigations. The same applies for asking a colleague for a second opinion to confirm the diagnoses.
6. A Grid system can be expanded to an advanced e-learning (e-teaching) system as well as to associated electronic publication with automated referencing to medical library search and demonstration systems (PubMed) (5, 10).

The described world of an integrated network tissue – based diagnosis still seems to be a fiction far away from the daily workload of a pathologist. However, we should keep in mind, that several important tools to build such a system have already been developed and tested (10, 16, 18). To our experience, they work well and fulfill the expectations. Once, the fine tuning has been set up, the vision is its integration into a Grid, to provide satisfactory working environmental in solving difficult and highly computational problems.

ACKNOWLEDGEMENT

The financial support of the International Academy of telepathology, and of the Verein zur Förderung des biologisch – technologischen Fortschritts in der Medizin are gratefully acknowledged.

REFERENCES

[1] K. Kayser, B. Molnar, and R. Weinstein, *Virtual Microscopy: Fundamentals, Applications, Perspectives of Electronic Tissue-based Diagnosis*. Berlin: VSV Interdisciplinary Medical Publishing, 2006.

[2] K. Kayser, D. Radziszowski, P. Bzdyl, R. Sommer, and G. Kayser, "Towards an automated virtual slide screening: theoretical considerations and practical experiences of automated tissue-based virtual diagnosis to be implemented in the Internet," *Diagn Pathol*, vol. 1, p. 10, Jun 10 2006.

[3] K. Kayser and H. Hoffgen, "Pattern recognition in histopathology by orders of textures," *Med Inform (Lond)*, vol. 9, pp. 55-9, Jan-Mar 1984.

[4] K. Kayser, B. Kiefer, and H. U. Burkhardt, "Syntactic structure analysis of bronchus carcinomas - first results," *Acta Stereol*, vol. 4/2, pp. 249-253, 1985.

[5] K. Kayser and W. Schlegel, "Pattern recognition in histo-pathology: basic considerations," *Methods Inf Med*, vol. 21, pp. 15-22, Jan 1982.

[6] K. Kayser and H. J. Gabius, "Graph theory and the entropy concept in histochemistry. Theoretical considerations, application in histopathology and the combination with receptor-specific approaches," *Prog Histochem Cytochem*, vol. 32, pp. 1-106, 1997.

[7] K. Kayser, J. Görtler, K. Metze, R. Goldmann, E. Vollmer, M. Mireskandari, Z. Kosjerina, and G. Kayser, "How to measure image quality in tissue-based diagnosis (diagnostic surgical pathology)," *Diagnostic Pathology*, vol. 3(Suppl 1), p. S11, 2008.

[8] H. Tamura, S. More, and T. Yamawaki, "Texture features corresponding to visual perception," *IEEE Trans on Systems, Man, and Cybernetics (SMC)*, vol. 8, pp. 460-473, 1978.

[9] K. Voss and H. Süße, *Praktische Bildverarbeitung*. München, Wien: Carl Hanser Verlag, 1991.

[10] J. F. O'Callaghan, "An alternative definition for neighborhood of a point.," *IEEE TRans. Comput*, vol. 24, pp. 1121-1125, 1975.

[11] G. Voronoi, "Nouvelles applications des paramêtres continus à la théorie des formes quadratiques, dexièmes memoire: recherches sur les parallèloedres primitifs," *J Reine Angew Math*, vol. 134, pp. 188-287, 1902.

[12] G. A. Meijer, S. G. Meuwissen, and J. P. Baak, "Classification of colorectal adenomas with quantitative pathology. Evaluation of morphometry, stereology, mitotic counts and syntactic structure analysis," *Anal Cell Pathol*, vol. 9, pp. 311-23, Dec 1995.

[13] P. J. van Diest, K. Kayser, G. A. Meijer, and J. P. Baak, "Syntactic structure analysis," *Pathologica*, vol. 87, pp. 255-62, Jun 1995.

[14] K. Kayser and G. Kayser, "Virtual Microscopy and Automated Diagnosis " in *Virtual Microscopy and Virtual Slides in Teaching, Diagnosis and Research*, J. Gu and R. Ogilvie, Eds. Boca Raton: Taylor Francis, 2005.

[15] M. Oger, P. Belhomme, J. Klossa, J.-J. Michels, and A. Elmoataz, "Automated region of interest retrieval and classification using spectral analysis," *Diagnostic Pathology*, vol. 3 (Suppl 1), p. S17, 2008.

[16] R. R. Coifman, S. Lafon, A. B. Lee, M. Maggioni, R. Nadler, F. Warner, and S. W. Zucker, "Geometric diffusions as a tool for harmonic analysis and structure definition of data: Diffusion maps," *Proc Natl Acad Sci U S A.* . , vol. 102:, pp. 7426-7431, 2005.

[17] J. Gortler, M. Berghoff, G. Kayser, and K. Kayser, "Grid technology in tissue-based diagnosis: fundamentals and potential developments," *Diagn Pathol*, vol. 1, p. 23, 2006.

[18] K. Kayser, K. Metze, D. Radziszowski, S. A. Hoshang, T. Goldmann, Z. Kosjerina, M. Mireskandari, and G. Kayser, "Texture and object related automated information analysis in histological still images of various organs," *Analytical and Quantitative Cytology and Histology*, vol. in press, 2008.

[19] K. Kayser, J. Görtler, F. Giesel, and G. Kayser, "How to implement grid technology in tissue-based diagnosis: diagnostic surgical pathology," *Expert Opin. Med. Diagn.*, vol. 2, pp. 323-337, 2008.

[20] Y. Yagi and J. R. Gildertson, "A relationship between slide quality and image quality in whole slide imaging (WSI)," *Diagnostic Pathology* vol. 3(Suppl 1), p. S12, 2008.

[21] K. Kayser, J. Görtler, T. Goldmann, E. Vollmer, P. Hufnagl, and K. Gian, "Image standards in Tissue-Based Diagnosis (Diagnostic Surgical Pathology)," *Diagnostic Pathology*, vol. 3, p. 17, 2008.

[22] M. Mireskandari, G. Kayser, P. Hufnagl, T. Schrader, and K. Kayser, "Teleconsultation in diagnostic pathology: experience from Iran and Germany with the use of two European telepathology servers," *J Telemed Telecare*, vol. 10, pp. 99-103, 2004.

[23] H. J. Gundersen, T. F. Bendtsen, L. Korbo, N. Marcussen, A. Moller, K. Nielsen, J. R. Nyengaard, B. Pakkenberg, F. B. Sorensen, A. Vesterby, and et al., "Some new, simple and efficient stereological methods and their use in pathological research and diagnosis," *Apmis*, vol. 96, pp. 379-94, May 1988.

[24] H. J. Gundersen, "Stereology of arbitrary particles. A review of unbiased number and size estimators and the presentation of some new ones, in memory of William R. Thompson," *J Microsc*, vol. 143 (Pt 1), pp. 3-45, Jul 1986.

[25] M. Bibbo, D. H. Kim, T. Pfeifer, H. E. Dytch, H. Galera-Davidson, and P. H. Bartels, "Histometric features for the grading of prostatic carcinoma," *Anal Quant Cytol Histol*, vol. 13, pp. 61-8, Feb 1991.

[26] C. Germain, V. Breton, P. Clarysse, Y. Gaudeau, T. Glatard, E. Jeannot, Y. Legre, C. Loomis, I. Magnin, J. Montagnat, J. M. Moureaux, A. Osorio, X. Pennec, and R. Texier, "Grid-enabling medical image analysis," *J Clin Monit Comput*, vol. 19, pp. 339-49, Oct 2005.

[27] W. Johnston, D. Gannon, and B. Nitzberg, "Grids as production computing environments: The engineering aspects of NASA's information power Grid.," *Eighth IEEE International Symposium on High Performance Distributed Computing, Redondo Beach, CA, August 1999*, vol. IEEE Computer Society Press: Los Alamitos, CA,, 1999.

[28] T. Akiyama, Y. Teranishi, K. Nozaki, S. Kato, S. Shimojo, S. T. Peltier, A. Lin, T. Molina, G. Yang, D. Lee, M. Ellisman, S. Naito, A. Koike, S. Matsumoto, K. Yoshida, and H. Mori, "Scientific Grid activities and PKI deployment in the Cybermedia Center, Osaka University," *J Clin Monit Comput*, vol. 19, pp. 279-94, Oct 2005.

3D Imaging with WSI (Virtual Slide)

Yukako Yagi

Department of Pathology, Harvard Medical School, Boston, MA, USA

Background

In the past, most 3D imaging in Pathology was done from a single slide using multiple focal planes (via confocal microscopy or cytology) or through volume rendering of large, macro structures on multiple physical sections. However, WSI technologies and rendering software have now improved to the point that 3D reconstruction of large structures at microscopic scale from hundreds of serial sections is possible. There is now much demand for interface between 3D imaging of histology sections and other modalities such as CT scanning, endoscopy and TEM Indeed, 3D Imaging has the potential to bring about new discoveries in medicine. However, challenges remain: section registration, quality of tissue and the effects of tissue processing and sectioning all must be optimized, and the huge amount of data that can be generated must be processed, stored and made available as quickly and efficiently as possible.

Methods

Specimens included lymph node, pancreas, esophagus, stomach and mouse embryo. 66-200 serial sections were cut manually or by an automated sectioning machine (AS-200, KURABO INDUSTRIES LTD. Japan) from formalin-fixed paraffin-embedded blocks and stained with H&E. Pancreas and mouse embryo were cut by AS-200. Serial sections were scanned at 0.33um/pixel using a Mirax Scan device (3DHISTECH Ltd, Carl Zeiss Microimaging GmbH) or at 0.5um/pixel using a ScanScope XT device (Aperio, CA, USA). 3D reconstruction was done using Mirax software and in-house software based on Image J (NIH, USA). The in-house software was used as an adjunct to the Mirax Software. Due to the PC's operational limitations, a set containing over 100 slides was divided into multiple models (50-100 sections/model). The specification of the PC used to make and view 3D models was OS: Windows Vista Ultimate 64 bit, CPU: 2 Quad Processor 2.84GHz, RAM: 8GB DDR2, VIDEO Memory:1GB NVIDIA Ge Force 9800 GT . WSI were aligned to produce a 66-100 section 3D stack that could be sub-sampled, sectioned in various planes and freely rotated to expose 3D relationships in tissue. Spacing between scanned sections was varied dynamically during the analysis to explore specific features.

Results

Morphologic features were often enhanced upon 3D reconstruction, although the relatively low resolution of the 3D model precluded extensive analysis of cellular interactions. The reconstruction process was made more difficult by tissue processing effects such as wrinkle, stretch, bubble and variable thickness across the tissue section.

Total file sizes to create one 3D model were 50-100 GB/model. The average 3D model size was 100 MB.

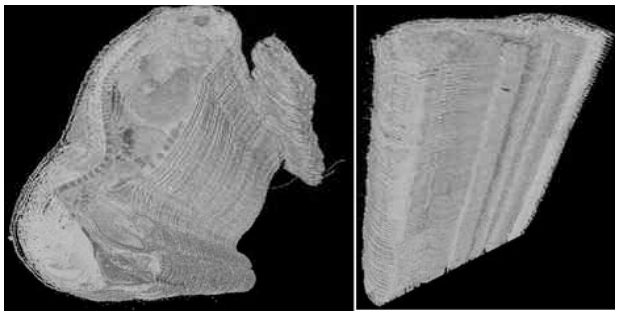

figure1

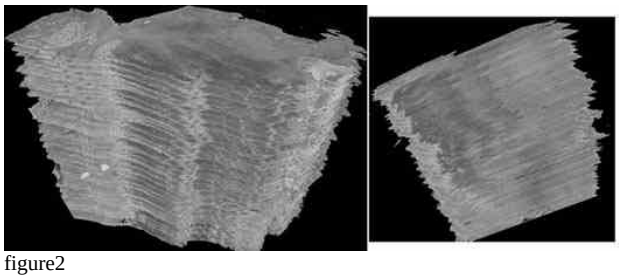

figure2

Figures 1 and 2 show the 3D models of mouse embryo and pancreas. Both sections were cut by AS-200. Because the quality of the slides was consistent and the thickness was uniform across each slide, it was relatively easy to produce acceptable 3D models. The mouse embryo was easier to align than other samples since it contains all organ systems with a variety of features. The pancreas model looks good at first glance. However, although the quality of the slide was consistent, the sliced plane shows some misalignments when the 3D model was sliced horizontally. All of the slides had some tissue wrinkles at exactly the same locations on each slide. The slides did not have enough features to align perfectly with low resolution by the algorithm.

Figure 3 shows the 3D models of follicular lymphoid. The sections were cut by hand. It is difficult even for experienced technicians to cut hundreds of serial sections.
Image A is a case of reactive follicular hyperplasia involving tonsil. Image B is a case of grade 1-2 out of 3 follicular lymphoma involving a lymph node. After alignment of serial sections and stacking of images, the relative amounts of cortex and paracortex and the features and patterns of the follicular structures in each case are emphasized.

A B

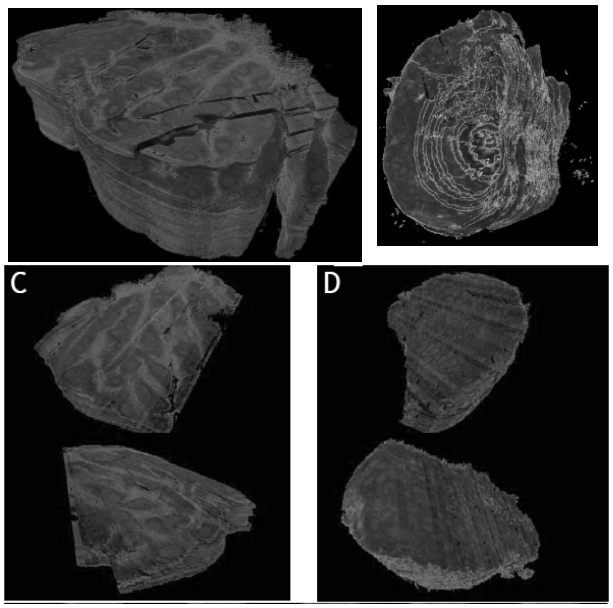

figure3

We found that the following technical issues need attention:
1. Registration must be done both by block and by slide
2. Slide quality must be consistent
3. Tissue features must be recorded by organ and tissue processing method
4. The size of spaces between slides must be measured.
5. Computer memory and performance must be optimized. The size of the original 2D images and the number of slides being processed resulted in compromised resolution on our standard departmental PCs, and the size of the 3D models made working with the models slower and more time-consuming.

Discussion

Our initials results show that 3D imaging using WSI could be extremely useful to pathologists in the near future. However, many technical issues remain to be addressed.
For example, twelve small 3D models of an esophageal cancer specimen were required to represent the resected tissue in its entirety and to see the coloration between endoscopic images. The endoscopic data alone, however, was not good enough to see the coloration
(It is important to be able to accumulate all necessary data from evaluate all accumulated data from other modalities such as CT.

Most importantly, we have found that no matter how thin or how uniformly we cut tissue specimens, there is always missing space between the slices. To be able to use 3D for image analysis or volume processing, development of a transformation algorithm for 3D reconstruction is necessary. To this end, we are looking into two possible methodologies.
The first would be to use Delaunay Triangulation to adjust the distortion caused by the tissue preparation gap between tissue sections. Based on Delaunay's definition, the circumcircle of a triangle formed by three points from the original point set is empty if it does not contain vertices other than the three that define it (other points are permitted only on the very perimeter, not inside). The Delaunay condition states that a triangle net is a Delaunay triangulation if all the circumcircles of all the triangles in the net are empty. This is the original definition of two-dimensional space. It is possible to apply this to three-dimensional space by using a circumscribed sphere in place of the circumcircle. The second possibility is to collect data on the exact shape and size of the tissue in each paraffin block, since usually the tissue embedded in the paraffin block is not visible. The combined use of these two methods has begun to show positive results in the initial data.

Conclusion

3D reconstruction from multiple serial WSI sections can be used to generate impressive views of tissue. In the future this technique could be an important aspect of pathological analysis. In addition, it will be very useful for educational purposes to be able to view and understand tissue structure in a 3D format. However, many challenges remain. Advanced 3D imaging research, as well as research aimed at solving the attendant technical issues, is ongoing at Massachusetts General Hospital.

3D nuclear cytometric feature analysis for renal cell carcinoma grading

H.J. Choi[1], T.Y. Kim[2], H.K. Choi[2]

[1]Center for Image Analysis, Uppsala University, Sweden,
[2]School of Computer Engineering, Inje University, South Korea
email: hyunju.choi77@gmail.com

***Abstract*—The aim of our study is to develop 3D nuclear cytometric features for quantitatively assessing the degree of malignancy and find an optimized classifier with the best discriminative power for renal cell carcinoma (RCC) grading. 3D nuclear cytometric features (3D nuclear morphometric features, 3D chromatin texture features, 3D nuclear surface texture features) were extracted. After dimensionality reduction of extracted features by principal component analysis (PCA), we made a classifier and assessed the significance by discriminant analysis. It yielded an accuracy of 82.59%. The results indicate the potential and feasibility of RCC grading using 3D nuclear cytometric features.**

***Index Terms*—Nuclear grading, Renal cell carcinoma, 3D nuclear morphometric features, 3D chromatin texture features, 3D nuclear surface texture features**

I. INTRODUCTION

Cytometry refers to the measurement (-metry) of cells (cyto-) and cellular constituents. These measurements may be of the physical properties of the cell, or of its biochemical properties, or of a combination of these. Digital image cytometry is to extract these cell properties from images using digital image analysis. It allows us not only to study the characteristics of the cell itself but also to study various substances inside the cell.

For diagnosis and prognosis of cancer, digital image cytometry has been performed on many studies to characterize the size, shape, DNA content of cells, and patterns of chromatin distribution in cell nuclei [1]-[4]. Their results showed that the limitations of qualitative evaluation could be overcome by using computer-assisted microscopic image analysis.

However, most of these studies used two-dimensional (2D) thin tissue sections which contained only partial cells. The truncation of cells during the sectioning process can lead to inaccurate quantification, as determining the size or shape of a cell depends on the angle of physical sectioning relative to the position of the cell. Therefore, to obtain clinically useful results, more accurate and reproducible methods are required.

According to the necessity of three-dimensional (3D) image analysis, several studies have investigated how to construct a 3D visualization and quantify 3D cytometric features from the volumetric data obtained from confocal laser scanning microscopy (CLSM). However, they focused only on the quantification of variations in nuclear size in three dimensions [5], [6]. Despite the potential advantages inferred from an amount of literature on the value of cytometric features for the detection of cancer, there are few studies on describing and quantifying nuclear appearance and chromatin pattern in three dimensions. Recently, 3D nuclear texture features were implemented to detect changes in nuclear chromatin patterns in thick tissue sections imaged by CLSM in a single study [7]. The aim of our study was to develop 3D nuclear cytometric features for quantitatively assessing the degree of malignancy and find an optimized classifier with the best discriminative power for renal cell carcinoma (RCC) grading.

II. MATERIALS AND METHODS

A. Specimen preparation and image acquisition

Eight cases of RCC were obtained from the Department of Pathology, Yonsei University College of Medicine. They had been fixed in 10% neutral-buffered formalin and embedded in paraffin before receipt. The tissues were cut into 20-μm sections, stained with propidium iodide (PI) containing RNase A (final concentration, 0.5 mg/mL), and mounted in a fluorescent mounting medium (DAKO, Carpinteria, California, USA). The RCC tissues were imaged with a TCS SP2 AOBS confocal imaging system (Leica Microsystems Ltd., Mannheim, Germany) equipped for Leica Dmire2 (Leica Microsystems Ltd., Mannheim, Germany), a 63x, 1.4 NA HEX PL-Apochromat objective lens(Leica Microsystems Ltd., Mannheim, Germany), and a HeNe laser.

We acquired a series of 2D optical sections, 0.4 μm apart, starting above the top surface of the section and extending down to the bottom surface. There were a total of 50 slices for each volume data, and each slice was a 24-bit/pixel image with a size of 512 × 512 pixels.

B. Segmentation and surface rendering of cell nuclei

In order to make 3D measurements on cell nuclei for RCC grading, first of all, the cell nuclei have to be segmented exactly. Once the cell nuclei have been segmented from each other and from the background,

nuclear cytometric features can be extracted from the individual cell nuclei. Next, surface rending is needed as a preprocessing step, since some of the 3D nuclear cytometric features that we define in this study are derived from 3D surfaces of the cell nuclei.

Segmentation of cell nuclei was done by the method proposed in our previously study [8]. We used Pun's method to segment cell nuclei. As the post processing of an initial segmentation, we corrected and removed any incorrectly segmented nuclei. To render 3D surfaces of cell nuclei, the marching cubes algorithm was used [9]. This algorithm produces a triangle mesh by computing isosurfaces from 3D data. By connecting the patches from all cubes on the isosurface boundary, we get a surface representation. Fig. 1 shows the results of the surface rendering for representative samples of cell nuclei for each grade.

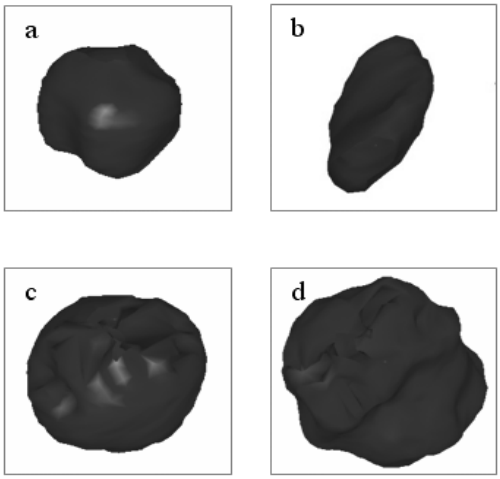

Fig.1. Surface-rendering images for cell nuclei of Grade 1 (a), Grade 2 (b), Grade 3 (c), and Grade 4 (d).

C. 3D nuclear morphometric features

Feature extraction is a crucial step in most cytometry studies; it defines what is to be measured and how the measurements will take place. Features selected for measurement should agree with a pathologist's view of what an important feature is.

Most RCC grading systems are based on morphonuclear criteria, such as nuclear size and shape [10]. In this respect, variations in nuclear size and shape can be important diagnostic factors, which can be expressed and quantified by morphometric features. We defined and extracted the 3D nuclear morphometric features as follows.

1) Volume: This is determined by the total number of voxels in the nucleus. The number of voxels multiplied by the size of a voxel gives the size of a cell nucleus in standard units.

2) Surface area: The area of a 3D cell nucleus can be approximated by the number of voxels belonging to the nucleus that have at least one neighboring background voxel. However, to find all the surface voxels, the relationships between voxels must be recomputed using the connectivity operation. We used Heron's formula as an alternate way to measure surface area, calculating the area of a triangle directly in terms of the lengths of the three sides, since the rendered surfaces consist of triangles in computer graphics. After calculating each of the triangle areas, we obtained the total surface area using the sum of all triangle areas.

$$S = \sqrt{s(s-a)(s-b)(s-c)} \quad (1)$$

where a, b, c are the lengths of the sides of a triangle and $s = (a+b+c)/2$.

3) Spherical shape factor: This represents how similar the shape of the cell nucleus is to a sphere. If A is the surface area of the nucleus and V is the volume of the nucleus, then the spherical shape factor is defined as:

$$36 \cdot \pi \cdot V^2 / A^3 \quad (2)$$

D. 3D chromatin texture features of cell nuclei

Chromatin pattern also plays a significant part in RCC grading [11]. The most widely used method for quantifying chromatin pattern is texture analysis, using gray level co-occurrence matrix (GLCM). The matrix contains an estimate of the joint probability density function for pixels separated by a particular number of rows, diagonals or columns. Texture features are derived from this matrix [12].

However, since GLCM only considers the spatial dependency of pixels on one image, there are some problems in extracting 3D chromatin texture features of cell nuclei using conventional GLCM. For example, if we process 3D volume data as individual 2D slices, some inter-slice information is ignored, increasing the possibility of data loss. To resolve such problems, we extended 2D GLCM to 3D GLCM that can quantify the 3D spatial dependency of voxel data on the object volume, which exists across several slices.

Similar to conventional GLCM, co-occurrence matrices for volume data are also represented by an $n^* n$ matrix in which n is the number of gray levels. These matrices are defined using the specific displacement vector $d = (dx, dy, dz)$ for each direction, where dx, dy, and dz are the number of voxels that move along the x-, y-, and z -axis, respectively. With respect to each voxel, voxels in 26 directions can be examined, but only 13 directions were considered to avoid redundancy.

If the co-occurrence matrix was calculated directly from the original image it would become very large, 256x256, and highly dependent on both the illumination level and contrast setting. To overcome this problem, we reduced the number of the gray levels to 64 and carried out a histogram equalization operation. And we computed GLCMs for 13 directions, and averaged them.

From the calculated matrix, we extracted 3D nuclear chromatin texture features: Contrast, Difference Moment, Inverse Difference Moment, Diagonal Moment, Second Diagonal Moment, Energy, Entropy and Uniformity.

E. 3D surface texture features of cell nuclei

Shape representation generally looks for effective and perceptually important shape features based on shape

boundary information. While tracking a contour in 2D images is easily done to extract boundary information, the extension to higher dimensions is nontrivial and requires the development of new concepts. In three dimensions, the boundary of an object can be defined as the surface, which is the physical boundary between the 3D object and the surrounding environment. The topological form of the surface is referred to as the surface texture.

After surface rendering, the surfaces of 3D cell nuclei consist of triangle meshes. Each triangle has a normal vector to the surface. The vector is perpendicular to the surface and the direction of the vector determines the orientation of the surface. The normal vectors for each triangle are yielded by the cross product of the two edge vectors on each triangle. The angles between adjacent normal vectors are obtained by the inner product.

$$n_i \cdot n_j = \cos(\theta_{ij}) \qquad \theta_{ij} = \cos^{-1}(n_i \cdot n_j) \tag{3}$$

where n_i is the unit normal vector to the triangle *i*, n_j is the unit normal vector to the triangle *j*, and θ_{ij} is the angle between triangles *i* and *j*.

Before computing the angles, we must consider the adjacency of triangles. It is necessary to store the adjacency relationships for each triangle to allow direct access to the adjacent triangles of any given triangle. We defined that adjacent triangles must share two vertices and made an adjacency list and a normal vector list containing information about the connectivity and the normal vector per triangle. From the lists, we computed angles between adjacent normal vectors and made an angle feature histogram. The angle feature histogram (AFH) is a histogram of the crease angles at the edges between adjacent triangles. This histogram can be defined as

$$h(\theta_k) = n_k \tag{4}$$

where θ_k is a crease angle and n_k is the number of triangles having the crease angle θ_k.

The angle θ_k varies between 0 and 180 degrees. The horizontal axis of the histogram plot was divided into 36 histogram bins of 5 degree. From the AFH, we extracted 3D nuclear surface texture features: AFH-Mean, AFH-Variance, AFH-Skewness, and AFH-Kurtosis.

F. Feature analysis and selection

Two approaches were used to find the set of features that maximizes the performance of the classifier for RCC grading. First, Sequential stepwise selection was adopted as a feature selection method. Stepwise selection combines forward and backward selection and repeats the addition and removal of a feature at each step. This method can overcome the nesting problem in which a decision cannot be changed when a feature is added or removed [13]. Through this method, the two most discriminating features were selected as candidates for creating a classifier, as shown in Table 1.

Table 1
Stepwise selection summary

Step	Variable Entered	F-Value	Pr>F
1	Volume	110.63	<.0001
2	AFH-Kurtosis	30.21	<.0001

As second feature selection technique, principal component analysis (PCA) was used to reduce the dimensionality of the features [14]. PCA is a standard decorrelation technique. The derived orthogonal projection basis leads to dimensionality reduction, and possible to feature selection. Based on the result of this analysis, the eigenvectors corresponding to the small eigenvalues were excluded and a total of three principal components were selected. Then, we used these three principal components as new features with the linear combination of each eigenvector and the original extracted feature values.

III. RESULTS

We implemented the proposed methods using Microsoft Visual C++ (Redmond, Washington, USA) and Open GL (Mountain View, California, USA). The total tested data set consisted of 324 cell nuclei. The number of cell nuclei for each grade was 80, 78, 94, and 72, respectively. A pathologist selected the tested data as representative samples of cell nuclei for each grade.

A. Significance assessment of 3D nuclear cytometric features

To evaluate what quantitative features of 3D analysis could contribute to diagnostic information and how it could increase the accuracy of nuclear grading, we analyzed the statistical difference of extracted 3D nuclear cytometric features among the grades. We used an analysis of variance (ANOVA) to determine the levels of statistical significance in the differences in distribution across the grades. For each test, we found the F-value as a result of the ANOVA. The F-value is the ratio of a between-group sum of squares (between-group variability) to a within-group sum of squares (within-group variability). Optimal features will have a high between-group variability compared to within-group variability. This means that the best feature will have the largest F-value. We found that volume is the best feature in grading.

B. Evaluation of classifier performance

Based on the minimum error rate classification of Bayesian decision theory [15], we created two classifiers using the feature set selected by stepwise selection and the new feature set made by PCA and compared the correct classification rate (CCR) for each classifier for a training data set and a test data set. 162 cell nuclei out of the total data set consisted of 324 cell nuclei were used to train classifiers and the rest were used to test the classifiers. Our comparison revealed that the CCRs were 78.55% and 82.59% for the classifier using the feature set selected by stepwise selection and the feature set generated by PCA,

respectively. The results showed that the classifier using the feature set by PCA provided better results for grading in Tables 2 and 3.

Table 2
Confusion matrix for the classifier using the feature set selected by stepwise selection

Grade	G1	G2	G3	G4	Total	%
G1	32	6	0	0	38	79.72
G2	5	29	9	1	44	75.31
G3	3	3	35	4	45	73.69
G4	0	1	3	31	35	85.48
Total	40	39	47	36	162	78.55

Table 3
Confusion matrix for the classifier using the feature set made by PCA

Grade	G1	G2	G3	G4	Total	%
G1	33	5	0	0	38	84.72
G2	7	31	9	1	48	80.15
G3	0	3	35	2	40	74.04
G4	0	1	3	33	36	91.45
Total	40	39	47	36	162	82.59

IV. DISCUSSION AND CONCLUSION

Nuclear grading is an important procedure in diagnostic pathology to assess the degree of malignancy from specimens of tumor tissue. In particular, the importance of nuclear grading in RCC has been reported, which is regarded to be strongly associated with prognosis and survival. However, the drawback of these studies is the most nuclei are not intact because of thin sections. It can result in potential loss of important information. Thus, in this study, we attempted to develop 3D nuclear cytometric features for RCC grading using 3D volume data imaged by CLSM.

The extracted features were divided into three categories: 3D nuclear morphometric features, 3D chromatin texture features and 3D nuclear surface texture features. Compared with 3D chromatin and surface texture features, the implementation of 3D nuclear morphometric features was less complex concerning mathematical modeling and computer algorithm. Whereas, 3D chromatin and surface texture analysis was complicated and required the development of new methods.

In the approach for describing 3D chromatin structure, the extension of GLCM to 3D could resolve the problem that inter-slice information is lost. It showed the possibility of extracting higher order statistical texture features from 3D grey level run length matrix (GLRLM) [16], and grey level entropy matrix (GLEM) [17].

The advantage of the triangle mesh descriptions for deriving 3D nuclear surface texture features is that missing data can be interpolated using smoothness. Compared with parametric surface description, it is more suited for the representation of most biological objects because structures in the microscopic scale typically show greater complexity. Moreover, the proposed 3D nuclear surface texture features are simple and easy to extract.

The set of 3D nuclear cytometric features defined in this study demonstrated its discriminating capability for four different grades of RCC. A new feature set by PCA yielded high classification accuracy in the discriminant analysis. However, some problems still remain. To improve the accuracy and reproducibility of RCC grading, we will seek suitable approaches and consider various classification models, such as a support vector machine (SVM), neural networks, and fuzzy methods, as well as statistical approaches. Additional studies on large number of cases have to be performed to validate our result and to evaluate for routine diagnostic procedures in histopathology.

REFERENCES

[1] H.K. Choi, T. Jarkrans, E. Bengtsson, J. Vasko, K. Wester, P.U. Malmstrom, C. Busch, "Image analysis based grading of bladder carcinoma; comparison of object, texture and graph based methods and their reproducibility," *Anal Cell Pathol*, vol.15, pp.1-18, 1997.

[2] C. Francois, C. Decaestecker, O.D. Lathouwer, C. Moreno, A. Peltier, T. Roumeguere, A. Danguy, J.L. Pasteels, E. Wespes, I. Salmon, R.V. Velthoven, R. Kiss, "Improving the prognostic value of histopathological grading and clinical staging in renal cell carcinomas by means of computer assisted microscopy," *J Pathol* ,vol.187, pp.313-320, 1999.

[3] E.C.M. Mommers, N. Poulin, J. Sangulin, C.J.L.M. Meijer, J.P.A. Baak, P.J. van Diest, "Nuclear cytometirc changes in breast carcinogenesis," *J Pathol*, vol.193, pp.33-39, 2001.

[4] L.A. West, R. Swartz, D. Cox, I.V. Boiko, A. Malpica, C. MacAulay, M. Follen, "Cytometric features of cell nuclei of adenocarcinoma in situ and invasive adenocarcinoma of the cervix," *Am J Obstet Gynecol*, vol.187, pp.1566-1573, 2002.

[5] K. Fugikawa, M. Sasaki, T. Aoyama, "Role of volume weighted mean nuclear volume for predicting disease outcome in patients with renal cell carcinoma," *J Urol*, vol.157, pp.1237-1241, 1997.

[6] K. Yorukoglu, S. Aktas, C. Guler, M. Sade, Z. Kirkali, "Volume-weighted mean nuclear volume in renal cell carcinoma," *Urol*, vol.52, no.1, pp.44-47, 1998.

[7] A. Huisman, L.S. Ploeger, H.F.J. Dullens, N. Poulin, W.E. Grizzle, P.J. Diest, "Development of 3D chromatin texture analysis using confocal laser scanning microscopy," *Cell Onco,l* vol.27 pp.335-345, 2005.

[8] H.J. Choi, H.K. Choi, "Grading of renal cell carcinoma by 3D morphological analysis of cell nuclei," *Comput Bio Med*, vol.37, pp.1334-1341, 2007.

[9] W.E. Lorensen, H.E. Cline, "Marching cubes: A high resolution 3d surface construction algorithm," *Comput Graph*, vol.21, pp.163–169, 1987.

[10] S.A. Fuhrman, L.C. Lasky, C. Limas, "Prognosis significance of morphologic parameters in renal cell carcinoma," *Am J Surg Pathol*, vol.6, pp.655-663, 1982.

[11] C. Francois, M. Remmelink, M. Petein, "The chromatin pattern of cell nuclei is of prognostic value for in renal cell carcinoma," *Anal Cell Pathol*, vol.16, pp.161-175, 1998

[12] R.M. Haralick, K. Shanmugam, I. Dinstein, "Textural Features for Image Classification," *IEEE Trans on Syst Man and Cybernet* , vol.3, no.6, pp. 610-624, 1973.

[13] H. Schulerud, G.B. Kristensen, K. Liestol, L. Vlatkovic, A. Reith, F. Albregtsen, H.E. Danielsen, "A review of caveats in statistical

nuclear image analysis," *Analyt Cell Pathol*, vol.16, pp. 63-82, 1998.
[14] R.A. Johnson, D.W. Wichern, Applied multivariate statistical analysis, 4th edn., Singapore: Prentice-Hall Inc., 1998.
[15] R.O. Duda, P.E. Hart, D.G. Stork, Pattern classification, 2nd edn, New York: John Wiley & Sons Inc., 2001.
[16] R.M.M. Galloway, "Texture analysis using gray level run lengths," *Comput Graph Image Process*, vol. 4, pp.172–179, 1975.
[17] K. Yogesan, T. Jorgensen, F. Albregtsen, K J. Tveter, H.E. Danielsen, "Entropy-Based Texture Analysis of Chromatin Structure in Advanced Prostate Cancer," *Cytometry*, vol.24, pp.268-276, 1996.

Hyun-Ju Choi is currently working as a postdoctoral fellow at Center for Image Analysis, Uppsala University, Sweden. She received her Ph.D. in Computer Science from Inje University, South Korea. Her research interest is computerized 2D and 3D image analysis using cells and tissues in vivo as well as in vitro.

Tae-Yun Kim is a Ph.D. student at the School of Computer Engineering, Inje University, South Korea.

Heung-Kook Choi is an Associate Professor at the School of Computer Engineering, Inje University, South Korea. He received both BS and MS degree in Computer Engineering at Linkoping University, Sweden in 1988 and 1990 respectively. His Ph.D. degree received in computerized image analysis at Uppsala University, Sweden in 1996. His interesting researches are computer graphics and medical image analysis.

A Pathological Image Retrieval Method Based on Local Medical Features

S. UENO[1], M. HASHIMOTO[1], R. KAWADA[1]
N. MIYOKAWA[2] and A. YOSHIDA[2]

[1]KDDI R&D Laboratories Inc., [2]Asahikawa Medical College
E-mail: sa-ueno@kddilabs.jp

Abstract— **In this paper, we propose a retrieval method for cancer biopsy images based on local medical features. The goal of this study is to retrieve past pathological cases that contain images that are similar to the current image in order to support doctor decisions.**

In the proposed method, we determine the medical features based on local structures of nuclei and glands such as the nucleus-cytoplasm ratio and the sizes of glands in the biopsy images. Subsequently, we calculate the statistical distributions of these local features as the biopsy image features. Those features are invariant to an object's position and rotation in images and are also capable of identifying similar biopsy images even if certain differences exist in the alignment of cells or the structures of glands. Next, we apply a post filtering method in order to improve the retrieval accuracy. For the retrieval, we select past query images from the database that are most similar to the current query image using the reconstructed feature spaces for the current query image. We search images using these feature spaces and eliminate dissimilar images from the retrieval results with a list of dissimilar images based on the feedback of previous pathologists.

Index Terms— **Information retrieval, Biomedical image processing**

I. INTRODUCTION

Stomach cancer has one of the highest mortality rates in Japan. Recently, around one hundred thousand patients suffer from this disease every year, with over fifty thousand patients dying of it each year in Japan [1]. With this in mind, it is essential for patients to obtain accurate diagnoses at an early stage. However, pathologists are hard-pressed to diagnose such diseases because of the lack of pathologists. In addition, in order to make an accurate diagnosis, they require a decision support system to assist them.

There are few studies concerning decision support systems using biopsy images of the stomach compared with other types of cancers, such as lung cancer [2][3], breast cancer [4][5], colorectal cancer [6] and prostate cancer [7]. Of these, most studies involving biopsy images to support pathologists focus on CAD (Computer-Aided Diagnosis). However, since many problems remain in making CAD systems capable of diagnosing as accurately as pathologists, we anticipate a large volume of research dealing with those systems. On the other hand, pathologists require a system showing images that resemble diagnostic images in terms of medical characteristics. Although there have been few such studies on decision support systems. It is useful for pathologists to seek similar images and findings previously diagnosed by doctors and such systems can help medical students to study using actual biopsy images.

In this paper, we propose a method for pathologists to support their diagnoses by showing similar pathology images using a retrieval system based on image features from a medical perspective and using relevant feedback. Although conventional methods have been studied for biopsy image retrieval based on visual features, such as color, texture, shape and so forth, these methods have problems; namely a failure to retrieve biopsy images by reflecting the perspective of pathologists. Therefore, we propose a biopsy image retrieval system that extracts medical features from diagnostic images. In the proposed method, we segment the biopsy images based on a medical perspective, extract the local medical features highlighted by pathologists by each block region and finally determine the distribution of these local medical features in the form of a query image feature. This method can retrieve biopsy images in various positions and rotations and is also capable of identifying similar biopsy images even if certain differences exist in terms of the alignment of cells or the structures of glands. Next, we apply a filtering method to improve the retrieval accuracy. For the retrieval, we select past query images from the database that resemble the current query image and eliminate dissimilar images from the retrieval results based on the feedback of previous pathologists.

In the next section, we introduce the features of biopsy images based on a medical perspective, while related works concerning the image retrieval system and the use of biopsy images are shown in Section III and our proposed method is described in more detail in Section IV. In Section V, we explain experiments involving biopsy image retrieval, before concluding our study in Section VI.

II. FEATURES OF GASTRIC CANCERS

In this section, we introduce the gastric biopsy image features, which are important for diagnosis, from reference [8]. To diagnose stomach cancer, doctors extract pieces of gastric mucosa during tests by gastro camera and create a section that is sliced about 5 μm thick after formalin fixation. Subsequently, they stain it with Hematoxylin Eosin (HE) staining and check it with a microscope. HE staining is used to dye the cell nuclei violet and the cell cytoplasm pink to facilitate a diagnosis.

We show an example of a biopsy image of normal mucosal tissue in Fig. 1. This figure shows three glands (dotted line regions), which indicate aggregations of cells specialized to secrete or excrete materials unrelated to their ordinary metabolic needs. The gland shape usually assumes a circular or elliptical form and pathologists diagnose whether the tumor is benign or malignant histologically via atypia. Atypia represents a morphological departure from normal tissue at the cellular and histological levels. Pathologists diagnose them from multidirectional perspectives, which can be divided into two broad categories. One is cellular atypism, with the focus on cellular size, shape and so forth. The other is structural atypism, with the focus on the alignments of cells, such as glands.

One of the most common measures of cellular atypism is the ratio of the nucleus in the cell cytoplasm (nucleus-cytoplasm ratio, N/C ratio), while one of the most common measures of structural atypism is the level of gland differentiation. Generally, the grade of cellular atypism can be identified by the magnitude of the N/C ratio. Moreover, structural atypism generally falls into three categories. Firstly, well-differentiated adenocarcinoma is the category in which we can recognize the shape of glands. Secondly, poorly-differentiated adenocarcinoma is the category in which we cannot recognize the shape of glands. Thirdly, moderately-differentiated adenocarcinoma is the category that lies midway between well- and poorly-differentiated adenocarcinoma. Fig. 2 shows examples of cellular atypism biopsy images, while Fig. 3 gives examples of structural atypism biopsy images. In Fig. 2, the nuclei are illustrated by the pink area (with cells enclosed by dotted lines and nuclei enclosed by red dotted lines). Fig. 2 (a) shows a normal gland, in which the sizes of the nuclei are about one third that of the cell. However, in Fig. 2 (b), the nuclei sizes are about half or more of that of the cell and with a long and thin shape. Likewise, Fig. 3 (a) shows well-differentiated adenocarcinoma, where we can recognize the normal shapes of the gland (via a dotted line). Moreover, Fig. 3 (b) shows poorly-differentiated adenocarcinoma, where we cannot recognize the shape of the gland cell.

III. RELATED WORKS

Many studies have been conducted on image retrieval systems based on image features. Therefore, in this section we explain related works focusing on general content based image retrieval methods and similar image retrieval methods for biopsy images.

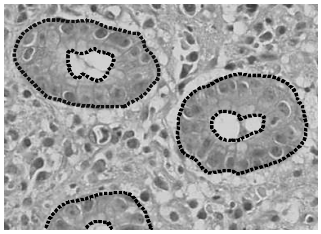

Fig. 1: Example of a gastric biopsy image. The dotted line regions are glands.

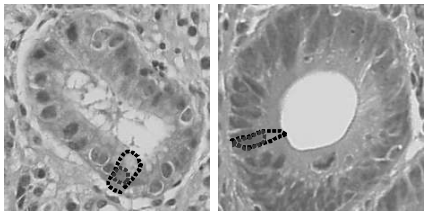

(a) Normal (b) Gastric adenoma

Fig. 2: Examples of cellular atypism. Each dotted line region is a cell and each red area is a nucleus.

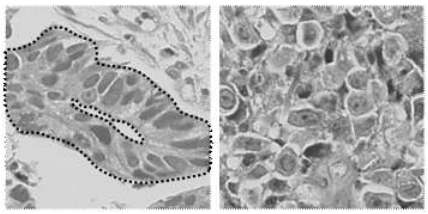

(a) Well-differentiated (b) Poorly-differentiated

Fig. 3: Examples of adenocarcinoma. The dotted line region is a gland region. We can recognize that there is no gland in Fig. (b).

A. Content-based similar image retrieval methods

Common similar image retrieval methods are based on visual image features. For example, color, texture and shapes [9] are applied. Common methods of image retrieval based on color use color histograms [10], which are effective features for representing images and effective in retrieving images of different color distributions from the database. On the other hand, for biopsy image retrieval, it is not very effective to use a color histogram, because the images in the biopsy image database have similar color distribution as a result of some staining processes as HE staining.

Common methods of image retrieval based on image texture are those using frequency-information [11]. It is effective for us to search images with a texture similar to the query image. However, for biopsy image retrieval, there is a problem retrieving similar images because these methods cannot reflect the perspective of the pathologist, such as the sizes of the nuclei and their arrangement.

When a common tendency of shapes is recognized in the database, it is useful to use the template matching method. For example, this method is used to detect the tumor shadow of breast cancer on CT images [12]. However, for biopsy image retrieval, it is difficult to determine certain common tendencies of nuclei and gland shapes, because their shapes vary depending on the operation to slice the biopsy at the process of section creation.

B. Related studies for pathology images

On another front, research regarding biopsy images has involved the study of image segmentation, which focuses on automated diagnosis of glands. Katsukura et al. proposed methods to extract gland regions on biopsy images [13][14]. He determines gland regions by repeating segmentation and integration, based on the tendency arrangement of glands. However, it is difficult to extract gland regions clearly as the cancer progresses, because there are no tendencies of the arrangement of glands on the cancer images. Tanaka et al. proposed a method to classify biopsy images into three categories, namely normal, adenoma and cancerous, using forty types of gland shape features and fourteen texture features [15]. However, they only used images from which the gland and nuclei regions could be extracted using his algorithm. Moreover, in their method, we need to choose rough gland areas manually. Zheng et al. created a system of biopsy image retrieval based on color histograms, texture, the Fourier transform coefficient and the wavelet transform coefficient [16]. However, they use only visual image features, meaning their methods cannot reflect the pathologists' perspective.

IV. PROPOSED METHOD

In this section, we propose a method for a pathology image retrieval system using diagnostic images based on local medical features. Moreover, we apply a post filtering method in order to improve the accuracy of the proposed retrieval method.

A. Image retrieval based on medical features

In this section, we show the method of image retrieval based on local medical features. The advantages of our method include the ability to segment an image into medical regions automatically using color features and then use the features from a medical perspective, that are invariant to position and rotation. The medical regions mean the gland regions, the nucleus regions and so forth. The flow of this method is shown in Fig. 4. Firstly, we segment a biopsy image into medical regions. Next, we extract the medical features from that segmented image. Then, we calculate the similarity between the query image and each image in a database, based on the distributions of local medical features. Finally, as the retrieval results, we show the images in order of similarity. The detailed process is described below.

1) Image Segmentation

In the proposed method, we segment an image into medical regions automatically using color features. Compared to the method described in [15], the benefit of our method is that pathologists do not need to segment gland regions from biopsy images manually. We segment a biopsy image into four medical regions, namely interstitium (A), glands (B), nuclei in the glands (C) and other background regions (D) from the medical perspective shown in Section II, in order to extract biopsy image features based on a medical perspective. Here, we call the region excluding the background interstitium (A). Fig. 5 shows the relationship of spatial inclusion among the regions. We extract each region in turn, from (A) to (C).

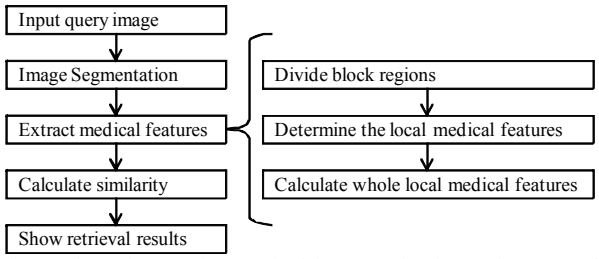

Fig. 4: Flow of processing required for extracting image features and image retrieval.

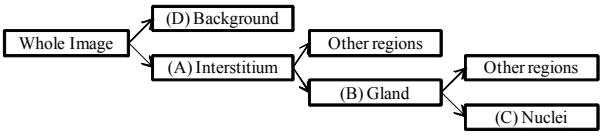

Fig. 5: Region categories. We segment a biopsy image into four regions.

We use a method using discriminant analysis based on color features. We use color features for the following reason: it is difficult to decide the representative shapes in each atypism because the shapes of each region usually differ dependent on the atypism in biopsy images. On the other hand, as each cellular region is colored similarly through HE staining, color features are less effective to identify atypism compared to shape features.

The flow of segmentation is shown below:

1. The whole image is divided into the interstitium (A) and the background region (D).
2. The interstitium (A) is divided into the gland (B) and other regions.
3. The gland (B) is divided into the nuclei (C) and other regions.

Firstly, we implement contrast emphasis and smoothing in order to segment the images robustly. We use gamma correction to emphasize contrast when we segment each of the regions. Furthermore, we use a median filter, which is capable of retaining the edge component and eliminate salt and pepper noise for smoothing. In this experiment, after using contrast emphasis, we repeat the process of median filter with 5x5 taps three times.

The background region (D) is virtually all white and usually smaller than other regions. Furthermore, white color saturation is lower than other regions; the interstitium (A), the gland (B) and the nuclei regions (C). Therefore, we first convert the color space from the RGB components into HSV components and in the S component we convert image binarization using Kittler's method [18], which involves the selection of a minimum error threshold. It is especially useful to divide the interstitium (A) from the background (D), because the sizes of the two regions differ considerably.

When we divide 2 class C_1, C_2, which is the interstitium (A) from the background (D) for the pixel value t, we determine the value of the threshold via the following

equation:

$$J(t) = w_1(t)\log\frac{\sigma_1(t)}{w_1(t)} + w_2(t)\log\frac{\sigma_2(t)}{w_2(t)} \quad (1)$$

In the equation, we determine $\omega_1(t)$ is the priori probability under t, $\sigma_1(t)$ is the standard deviation, while $\omega_2(t)$ is the priori probability over $t+1$ and $\sigma_2(t)$ is the standard deviation. If there is no background region in a query image, the value t remains potentially indeterminable. Therefore, we determine that there is no background region if the value t does not meet the requirement between $\mu - 2\sigma \le t \le \mu + 2\sigma$, where μ is the mean and σ is the standard deviation. We decide on this range via a preliminary experiment and herewith segment those two regions accurately.

In the next phase, we extract the gland region (B) from that interstitium region (A). (A) and (B), the interstitium and gland regions, differ in color through HE staining, since the gland region (B) takes on a blue tinge. Therefore, we convert the color space from RGB components into YCbCr components. Using Cb components, we determine a threshold to segment the image regions using Otsu's method [19]. When we divide 2 class C_1, C_2 which is the gland region (B) from interstitium region (A) on the pixel value t, we determine the value of the threshold via the following equation:

$$\sigma_B^2(t) = \frac{[\mu_T\omega_1(t) - \mu_1(t)]^2}{\omega_1(t)[1-\omega_1(t)]} \quad (2)$$

In the equation, we determine $\omega_1(t)$ is the priori probability under t, $\mu_1(t)$ is the mean while μ_T is the mean value in the whole image. We determine the value of the threshold t when $\sigma_B^2(t)$ peaks.

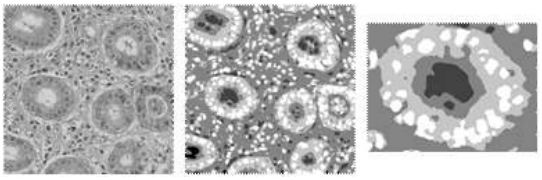

(a) Original (b) Segmented (c) Close-up

Fig. 6: Image Segmentation. The white areas are nuclei, the light gray regions are glands, and the gray regions are interstitium.

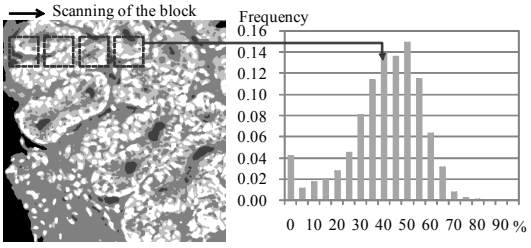

Fig. 7: An image of extracting image features. We split the segmented images into blocks, and calculate the features in each block. Subsequently, we calculate the histograms of distribution.

Finally, we extract the nuclei region (C) from that of the gland region (B). The nuclei region (C) is bluer than the gland region (B), so we convert the color space from RGB components into L*a*b* color components. Using b* components, we determine the threshold to segment the image regions using Otsu's method, just as in 1). Fig. 6 is an example of a segmented image where four regions were extracted from a medical perspective.

2) Extraction of the medical features

We introduce a method of extracting image features from the segmented images. Our proposed method uses a histogram of frequency distribution calculated for the local areas. Based on the pathologists' perspective shown in Section II, we calculate the following three features in each segmented block.

- Feature (α): N/C ratio, $\frac{(C)}{(B)}$.
- Feature (β): Ratio of the gland region in the interstitium, $\frac{(B)}{(A)}$.
- Feature (γ): Average size of the glands in each block.

Fig. 7 shows an example involving the calculation of feature vectors. We split the segmented pathology image into blocks and calculate those three features in each block. Subsequently, we determine the histograms of these individual features. The scanning of the block goes by pixel unit, whereupon we finally calculate the distribution of these local medical features. This method creates features invariant to position and rotation while reflecting a medical perspective.

3) Calculation of similarity

We determine vector data from the histogram as explained in 2). The feature vectors of images a and b are defined as $\mathbf{u}$ and $\mathbf{v}$, while the similarity of two vectors s is defined by the following expression:

$$s = \cos\theta = \frac{\mathbf{u}^T \cdot \mathbf{v}}{|\mathbf{u}||\mathbf{v}|} \quad (3)$$

Features (α), (β) and (γ) are normalized by their mean and standard deviation. Subsequently the overall image similarity is defined by linear combinations. The total image similarity is defined as follows,

$$D = \sum_i w_i s_i \quad (4)$$

In the equation, s_i is the similarity that is normalized and w_i is the weighting.

B. Improvement of retrieval results based on feedback

In this section, we apply a post filtering method in order to improve the retrieval accuracy. We select the most similar image from past query images. Next, we eliminate dissimilar images from the retrieval results based on the feedback of previous pathologists. (Fig. 8)

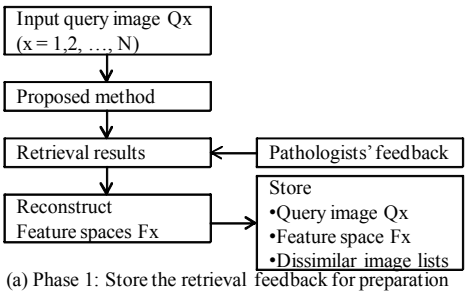

(a) Phase 1: Store the retrieval feedback for preparation

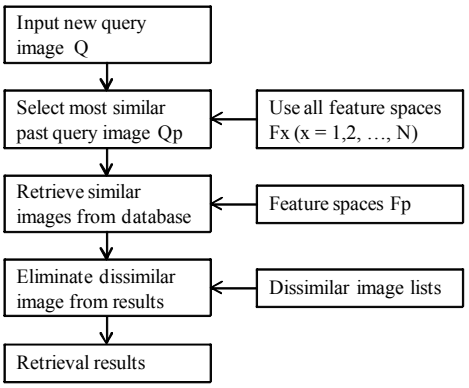

(b) Phase 2: Reflect the filtering based on feedback

Fig. 8: Process of filtering retrieval results

1) Reconstruction of feature spaces

In Phase 1 we decide the feature spaces F_x, which have similar images and dissimilar images split based on the relative Karhunen-Loeve transform method [20]. A Karhunen-Loeve transform can extract features that are contained in a category, but not contained in other categories. To decide the feature spaces F_x, we use the top N_r of results of images retrieved via the query Q_x.

It is probable that the retrieval images that pathologists have evaluated as similar are indeed similar to each other, so we use all of them to make a subspace. On the other hand, for dissimilar images, further analysis to generate a subspace is not required. We calculate the similarity between the query image Q_x and the subspaces of similar images using the multiple similarity method and compare the query image Q_x to dissimilar images using the cosine of the image vectors. We store these results for each query image Q_x, feature spaces F_x and dissimilar image list.

2) Reflection of the filtering based on feedback

In Phase 2, after searching N query images in Phase 1, we calculate the similarity between a new query Q and N past query images. Generally, we cannot decide the most suitable feature space of the new query Q before searching for it, so we search the most suitable feature space of Q using the past feature spaces of F_x using N past query images.

We determine the similarity between the new query image Q and past similar query images Q_x using all feature spaces of F_x. The certain feature space F_x for which one of Q_x is most similar to Q is defined as F_p and the corresponding Q_x is defined as Q_p. Alternatively, if there is no feature space F_x that satisfies the above assumption, we do not use this feedback method. In contrast, when we can obtain two or more feature spaces F_x we choose a feature space arbitrarily.

Next, we search for the similar images of Q using the feature space of F_p as explained above. Subsequently, we eliminate dissimilar images determined by the pathologists, based on the past query image Q_p from the retrieval results. This method is based on the black-list method.

V. EXPERIMENTS

A. Experimentation environment

One of the gastric criteria for diagnosis is Group classification [1]. As the disease progresses, it has five categories, namely Groups I, II, III, IV and V. Table 1 shows the Group classification.

Table 1: Group classification in gastric criteria

Group I	Normal tissue and benign lesion
Group II	Benign lesion with aberrant tissue
Group III	Boundary case between benign and malignant
Group IV	Tissue at increased risk for cancer
Group V	Complete cancer

In this experiment, we evaluate the retrieval methods using two pathologists (Drs. X and Y). Firstly, we register biopsy images in the database. This database consists of samples from twelve patients, where each patient has six biopsy images, making a total of seventy-two images. These images are checked by Doctor X and assigned into five Groups. Each of Groups I to IV has twelve images, while Group V has twenty-four images. Within Group V, the images are classified into two categories, as shown in Section II, namely well-differentiated adenocarcinoma and poorly-differentiated adenocarcinoma. In this paper, we define poorly-differentiated adenocarcinoma as GroupV:1 and well-differentiated adenocarcinoma as GroupV:2. The images have a resolution of 512×512 pixels and were captured through a microscope at two hundred times magnification. Moreover, two pathologists evaluate the similarity of images within the database, evaluating on a 5-point scale where any pair of images over 4-points are similar. The results of evaluation by Drs. X and Y were not very different. The evaluation of the retrieval approach is based on the precision-recall curve and we calculate an average precision of 11-points [21]. This variable indicates the number of retrieval results with the precision and recall defined as follows:

$$\text{Precision} = \frac{\left|\{\text{relevant images}\} \cap \{\text{retrieved images}\}\right|}{\left|\{\text{retrieved images}\}\right|} \quad (5)$$

Table 2: Retrieval results by Drs. X and Y. We compare the proposed method to seven other common methods with an average precision of 11-points by two pathologists.

		Doctor X	Doctor Y
	Proposed method	0.69	0.68
(α)	N/C ratio	0.62	0.62
(δ)	Color Histogram	0.60	0.55
(ε)	DCT	0.48	0.48
(ζ)	DWT	0.34	0.37
(η)	Color Layout	0.42	0.38
(θ)	Edge Histogram	0.28	0.29
(ι)	SIFT	0.42	0.37

$$\text{Recall} = \frac{\left|\{\text{relevant images}\} \cap \{\text{retrieved images}\}\right|}{\left|\{\text{relevant images}\}\right|} \qquad (6)$$

B. Image retrieval based on medical features

1) Decision of each feature space

Our proposed method involves dividing the images into local blocks, from which we can extract features. Under a constant power microscope, there are assumed to be certain relationships between the optimized sizes of block S_b, the average size of the nuclei and the average size of the glands, which represent the parameters of image features. Therefore, we experiment with the relationship between feature spaces, such as the block sizes and the retrieval accuracy using three features shown in Section IV.A.2). In this experiment, we use twenty queries from Groups II to V and evaluate using an average precision of 11-points. The reason why we do not use query images from Group I is that Group I is in the category of normal, benign tumors, making it less important for pathologists to search. Due to the lack of similar images in the database, we eliminate the query images from Group I.

Based on the preliminary experimental results, there is little difference between the evaluations of Drs. X and Y. The adequate sizes of S_b are about ten for Feature (α) and about twenty five for Features (β) and (γ), respectively. Furthermore, Feature (α) is the most accurate retrieval feature within the three proposed features. In this case, where the images are observed with a microscope at two hundred times magnification, the average size of a normal nucleus is about 10 × 10 to 20 × 20 pixels as a visual reference, while the gland regions are usually larger than the nucleus regions. We can recognize that the sizes of blocks on Feature (β) and (γ) are larger than the size of Feature (α). In the following experiments, we use these feature spaces.

2) Subjective evaluation

In this section, we combine the three features and optimize the feature spaces, which are shown in section IV.A.2) and in equation (4), to improve the accuracy of the retrieval system. We decide the weights w_i of features by the stepwise method [15] using ten queries from Groups II to V. In this experiment, weighting parameters were selected to have the optimal setting from the preliminary experiment. The selected parameters are shown in the following equation:

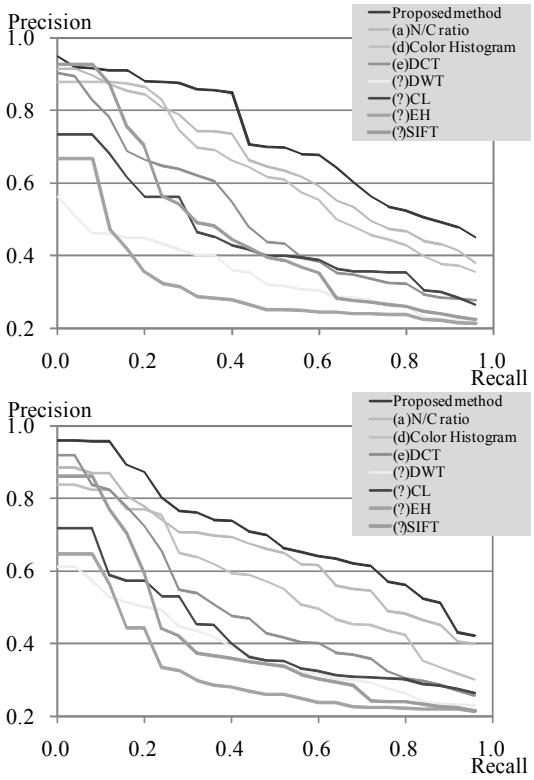

Fig. 9: Results obtained by the different method algorithms for precision-recall curves. The upper one is the results by Doctor X and the bottom one is by Doctor Y.

$$\omega_\alpha = 20, \omega_\beta = 1, \omega_\gamma = 1 \qquad (7)$$

Compared with our proposed method, we only use Feature (α), the most accurate of our proposed features. As Color Histogram is one of the most useful features for image retrieval, we use these features.

- Feature (δ): Color Histogram using the whole area of images [10]
- Feature (ε): DCT coefficients
- Feature (ζ): DWT coefficients [16]

These features are frequency information. Additionally, we use some MPEG-7 [24] features.

- Feature (η): Color Layout (CL)
- Feature (θ): Edge Histogram (EH) [25]

Lastly, we use one of the most common local features:

- Feature (ι): SIFT (Scale Invariant Feature Transform) [26]

In this experiment, we use twenty query images from Groups II to V. These query images differ from those used for optimizing the feature spaces.

Table 2 shows the average precision of 11-points of the retrieval results for each method, while Fig. 9 shows the precision-recall curves of the retrieval results for each method. In this table and figure, we can confirm that the proposed method is around a 15% improvement compared to other conventional visual feature methods and we conclude that our method is effective for biopsy image retrieval. Moreover, detailed results for each of the group images are shown in Table 3. In this table, we conclude that our method improves similar image retrieval, especially for retrieval on Group V.

In the proposed method, Feature (α) is quite effective to realize accurate retrieval. When we search for images, it is more accurate to use Features (α) to (γ) than Feature (α) alone. In particular, it is more effective in Group V:1 to use Feature (β) and Feature (γ). The reason why these features are effective for Group V:1, poorly- differentiated adenocarcinoma, is that there are small glands or no glands. Hence, calculating the ratio of the gland or its average size is important. In addition, when the uses of Features (δ) and (ε) are compared, Features (ζ), (η) and (θ) show less accurate results. This is because positional information of the glands or the nuclei reflected in Features (ζ), (η) and (θ) is not necessarily important from the perspective of pathology image retrieval. We could use Feature (ι), SIFT, when we want to get an image that is almost the same as the query image, but it is difficult to search a similar but slightly different image.

C. Filtering retrieval results based on feedback

On the practical side, we made an improvement to our proposed method that we demonstrated before, using the feedback of pathologists and filtering. Firstly, we determine a feature space for each query image. Next, we use a filtering method to eliminate images that were determined to be dissimilar to past query images by pathologists.

1) Evaluation experiments

In these experiments, we use the parameters $N = 20, N_r = 20, N_n = 10$, which are shown in section IV.B and determined from the preliminary experimental results. There are twenty images that were evaluated by two pathologists, while a new query image was selected using the leave-one-out method. Therefore, we evaluate twenty patterns of query images and the evaluation method involves the average precision and recall curves. The reason why we use the precision and recall evaluations to evaluate these retrieval systems is to confirm the accuracy in top placements in search results.

2) Experimental results

We show the retrieval results in Fig. 10 and evaluate the precision and recall based on the number of retrieval images. In this experiment, we confirm that for both pathologists' evaluations, we can improve the accuracy of the retrieval results. Especially when the number of retrieval images is less than 10, we can confirm the accuracy improvement in terms of both precision and recall. These results are important for pathologists because accurate retrieval based on reduced retrieval volumes help them to make a diagnosis. For example, where there are five retrieval images, the average precision is improved by 20% (Doctor X) and 18% (Doctor Y), while the average recall is improved by 13% (Doctor X) and 11% (Doctor Y).

Furthermore, we show an example of the retrieval results in Fig. 11. In Fig. 11, the query image (q) is a cancer image in Group V, with well-differentiated adenocarcinoma. In this Figure, (b-4) and (b-5) are dissimilar to query image (q). By contrast, (a-1) to (a-5) are all similar to query image (q). The figures show that retrieval using filtering based on the relevant feedback is useful to improve the accuracy of results.

Table 3: Retrieval results by query image groups. We compare the proposed method to seven other common methods with an average precision of 11-points by two pathologists. The upper one shows the results by Doctor X and the bottom one those of Doctor Y.

		II	III	IV	V:1	V:2
	Proposed method	0.61	0.77	0.67	0.82	0.58
(α)	N/C ratio	0.56	0.76	0.68	0.68	0.45
(δ)	Color Histogram	0.69	0.75	0.66	0.68	0.31
(ε)	DCT	0.55	0.46	0.47	0.67	0.26
(ζ)	DWT	0.13	0.46	0.45	0.50	0.13
(η)	Color Layout	0.38	0.54	0.51	0.47	0.22
(θ)	Edge Histogram	0.22	0.34	0.35	0.24	0.26
(ι)	SIFT	0.42	0.51	0.58	0.30	0.30

		II	III	IV	V:1	V:2
	Proposed method	0.50	0.80	0.64	0.90	0.57
(α)	N/C ratio	0.49	0.81	0.64	0.73	0.44
(δ)	Color Histogram	0.41	0.79	0.74	0.62	0.21
(ε)	DCT	0.48	0.52	0.48	0.70	0.26
(ζ)	DWT	0.23	0.60	0.38	0.51	0.08
(η)	Color Layout	0.26	0.58	0.42	0.47	0.22
(θ)	Edge Histogram	0.37	0.34	0.34	0.24	0.18
(ι)	SIFT	0.32	0.46	0.61	0.30	0.19

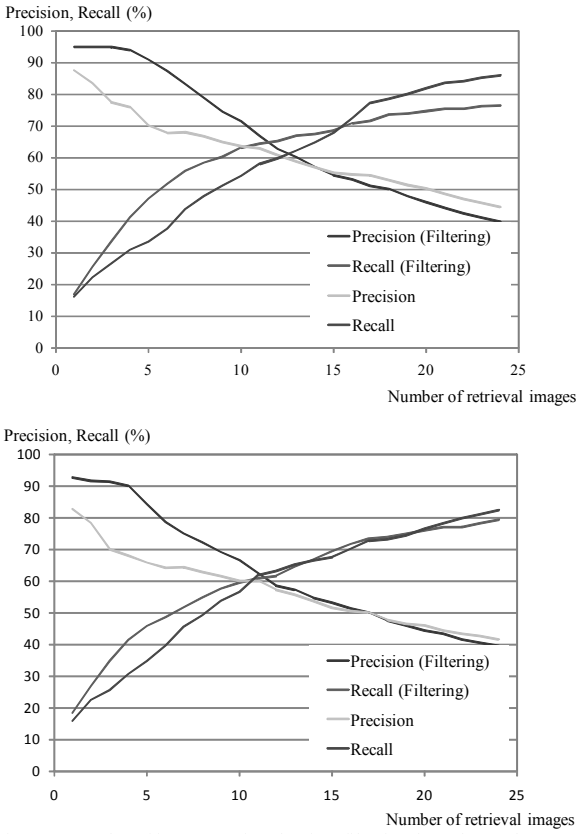

Fig. 10: Results of image retrieval using filtering based on relevance feedback method. The upper one is the results by Doctor X and the bottom one is by Doctor Y.

VI. CONCLUSION

In this paper, we proposed a new retrieval method for similar biopsy images based on local medical features. In the proposed method, we determine medical features, which are based on local structures of nuclei and glands.

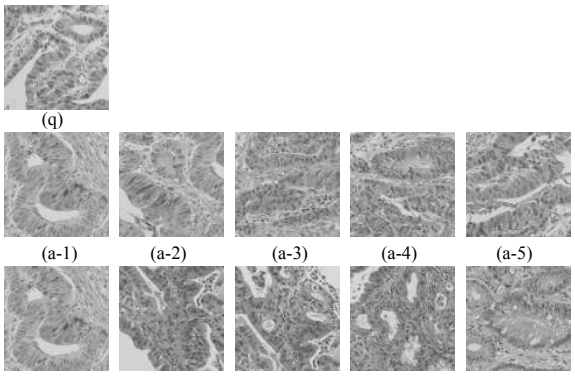

Fig. 11: Example of result of retrieval using filtering based on relevant feedback. (q) is a query image. (a-1) to (a-5) are the results of retrieval using filtering, (b-1) to (b-5) are the results of retrieval without filtering. The number (1-5) is retrieval sequence.

Subsequently, we calculate distributions of these local medical features for biopsy images. These features are invariant to position and rotation and are also capable of identifying similar biopsy images even if certain differences exist in the alignment of cells or the structures of glands. Next, we apply a post filtering method in order to improve the accuracy of the top rank in search results. For the retrieval, we choose a past query image from the database that is most similar to the current query image using the reconstructed feature spaces of the current query image. We eliminate images that are dissimilar to the query image from the retrieval results based on the feedback of pathologists. This method can improve the accuracy of retrieval.

The proposed method can be applied to other digestive organs such as the colon, small intestine and duodenum, etc. There are many similarities in these digestive organs from a medical perspective.

Our method is based on the N/C ratio and the features of glands. However, pathologists diagnose all the features of images, i.e., they also consider things from other medical perspectives. To improve the retrieval accuracy and deal with many types of biopsy images, other features are to be investigated for inclusion.

ACKNOWLEDGMENT

We would like to thank Dr. Masahiro Yamamoto for providing the image database and evaluating the retrieval method. In addition, we thank Drs. Fumiaki Sugaya, Shuichi Matsumoto and Shigeyuki Akiba, all at KDDI R&D Labs, for their various support and encouragement throughout this study.

REFERENCES

[1] E. Sekizuka. Gastric cancer. In A guideline of the clinical inspection, pages 158-163. Japanese Society of Laboratory Medicine, Tokyo, 2005.

[2] Y. Ukai, N. Niki, H. Satoh and S. Watanabe. Computer assisted images based on helical CT images. IEICE TRANS. INF. & SYST., J83-D-II (1):342-250, Jan. 2000.

[3] L. Rai, S. A. Merritt and W. E. Higgins. Real-time image-based guidance method for lung-cancer assessment. Computer Vision and Pattern Recognition, 2:2437-2444, Oct.2006.

[4] Y. Hagihara, Y. Hagihara and J. Wei. The advancement of CAD system for breast cancers by improvement of classifiers. IEICE TRANS. INF. & SYST., J87-D-II (1):197-207, Jan. 2004.

[5] P. S. Rodrigues, G. A. Giraldi and R. F. Chang. Non-extensive entropy for CAD systems of breast cancer images. In Computer Graphics and Image Processing, pages 121-128, Manaus Oct. 2006.

[6] R. L. V. Uitert, J. Li and R. M. Summers. Computer-aided detection of colonic diverticular disease. In Biomedical Imaging, pages 1244-1247, Washington DC, Apr. 2007.

[7] T. Saito, N. Otsubo, J. Toriwaki, H. Watanabe, K. Yokoyama and A. T. Takamatsu. A preliminary study on prostate cancer detection using microscope images of prostatic needle biopsy tissues stained with PSA. IEICE TRANS. INF. & SYST., J83-D-II (1):228-236, Jan. 2000.

[8] K. Nakamura. The structure of stomach cancer. IGAKU-SHOIN Ltd., Tokyo, 2005.

[9] K. Kushima, H. Akama, S. Konya and M. Yamamuro. Content based image retrieval techniques based on image features. Transactions of Information Processing Society of Japan, 40(SIG3 (TOD1)):171-184, Feb. 1999.

[10] M. J. Swain and D. H. Ballard. Indexing via color histograms. Computer Vision, 2:390-393, Dec. 1990.

[11] A. Laine and J. Fan. Texture classification by wavelet packet signatures. IEEE Trans. on Pattern Analysis and Machine Intelligence, 15(11):1186-1191, Nov. 1993.

[12] T. Nakagawa, T. Hara and H. Fujita. An image retrieval method using local pattern matching. IEICE TRANS. INF. & SYST., J85-D-II (1):149-152, Jan. 2002.

[13] K. Taniguchi, Y. Higashiwaki and T. Katsukura. A procedure for extracting gland tubules in tissue image of the stomach. IEICE TRANS. INF. & SYST., J70-D (6)1242-1427. Jun. 1987.

[14] T. Katsukura, T. Iida and K. Taniguchi. A new procedure for extracting gland tubules in a tissue image of the stomach. IEICE TRANS. INF. & SYST., J71-D (1):176-181, Jan. 1988.

[15] T. Tanaka, Y. Uchino and T. Oka. Classification of gastric tumors using shape features of gland. IEEE TRANS. EIS, 126(10):1242-1248, Oct. 2006.

[16] L. Zheng, A. W. Wetzel, J. Gilbertson and M. J. Becich. Design and Analysis of a Content-Based Pathology Image Retrieval System. IEEE TRANS. INFORMATION TECHNOLOGY IN BIOMEDICINE, 7(4):249-255, Dec. 2003.

[17] J. Z. Wang, G. Weiderhold, O. Firschein and S. X. Wei. Content-based image indexing and searching using Daubechies' wavelets. Int. J. Digital Libraries (IJODL), 1(4):311-328, Mar. 1998.

[18] J. Kittler and J. Illingworth. Minimum error thresholding. Pattern Recognition, 19(1):41-47, 1986.

[19] N. Otsu. An automatic threshold selection method based on discriminant and least squares criteria. IEICE TRANS. INF. & SYST., 63-D (4):349-356, 1980.

[20] Y. Ikeno, Y. Yamashita and H. Ogawa. Pattern recognition by Relative Karhunen-Loeve Transform Method. IEICE technical report. Pattern recognition and understanding, 95(583):17-22, 1996.

[21] T.G. Kolda and D.P. O'Leary. Latent Semantic Indexing via a Semi-Discrete Matrix Decomposition. Institute for Mathematics and Its Applications, (107):73-80, 1999.

[22] P. A. Maragos and R. W. Schafer. MORPHOLOGICAL SKELETON REPRESENTATION AND CODING OF BINARY IMAGES. Acoustics, Speech, and Signal Processing, IEEE International Conference, (9):523-526, Mar. 1984.

[23] G. N. Wang, M. Evens and D. B. Hier. On the evaluation of LITREF: a PC-based information retrieval system to support stroke diagnosis. Computer-Based Medical Systems. 1990., Proceedings of Third Annual IEEE Symposium, pages 548-555, Jun. 1990.

[24] ISO/IEC/JTC1/SC29/WG11: "MPEG-7 XM Document: MPEG-7 Visual Part Experimentation Model Version 10.0," *MPEG Document N4063*, Singapore, Mar. 2001.

[25] C. S. Won, D. K. Park, P. S. Jun. Efficient use of MPEG-7 Edge Histogram Descriptor. ETRI Journal. vol.24 No.1 pp.23-30, 2002.

[26] D. G. Lowe. Distinctive image features from scale invariant keypoints. International Journal of Computer Vision, 60, 2, 2004.

Network/data structure for WSI clinical usage

Yukako Yagi

Department of Pathology, Harvard Medical School, Boston, MA, USA

Background

Whole slide imaging (WSI) is entering the mainstream of Digital Pathology. Because it will be a key factor in determining the future direction of Digital Pathology, all aspects of WSI must be studied.. Many articles on scanning and display methods have been published, dealing with issues of image quality, clinical implementation, standardization, etc. However, there have been relatively few studies of network, system and data structure. IT technologies such as computer performance and operating systems are improving daily; at the same time, network security rules within institutions are becoming daily more complex. These factors make it more difficult to design an optimized WSI system and network for both internal and external use. In addition, the data structure of the WSI application, including 3D reconstruction, multilayer structure observation and multispectral imaging, has become more complex, with the result that WSI is now similar in concept to "series" of radiological images. Soon WSI will require a new type of data format.

In this paper, we discuss our primary findings on network, system structure, and WSI viewer performance, in order to provide information which might be useful to other institutions in building their own WSI network.

Methods and Materials

Materials:

Four different types of WSI scanners were installed in the Massachusetts General Hospital (MGH) Imaging Laboratory. Each scanner has a different system structure and a different data format over the internet or intranet. Most pathologists at MGH use very similar PC specifications: the OS is generally Microsoft Windows XP Professional version 2002 Service Pack 3 and CPU is Intel Core 2 CPI 6300 1.86GHz with 1GB of RAM. Some of the PCs have 2GB of RAM.

The network bandwidth in each office is either 0MB/s, 100MB/s or 1GB/s, although 1GB/s is very rare. The MGH Imaging Lab has over 5TB of WSI library scanned, with multiple scanners for multiple purposes. The images are used for education, conferences, image analysis, image analysis algorithm development, multispectral whole slide imaging research, 3D imaging, multilayer cytology, fluorescence and so on. The storage server is Quad-Core-2.33 GHz Zeon Processors, 18GB of memory, and 5TB SAS RAID array; OS is Windows 2003 server. Four types of WSI Server software run on the storage server machine. All scanners are connected to the storage server by 1 GB through the network switcher. The storage server is connected to the institution network by 4GB + 1GB through the network switcher. This prevents slowdown between the scanner and the storage server during scanning. Recently a 5 TB Network Hard Drive was added to optimize storage capability.

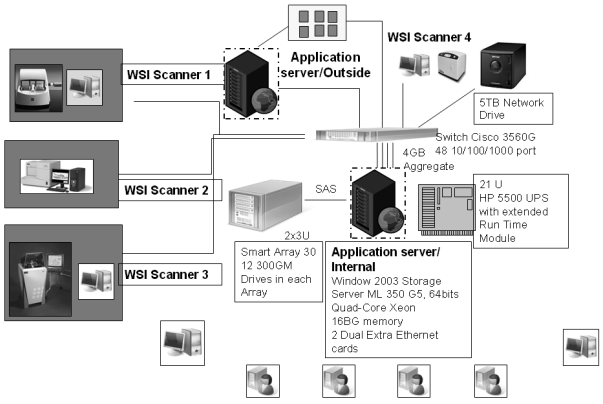

Figure 1

Figure 1 shows the system structure in the Lab.

In this setting, we examined network and GUI performance for different purposes under varying conditions. All viewers were simple, open HTTP message interface, to enable client software to incrementally access image information and data views from virtual slides.

Methods:

The following uses were tested:

Two of the MGH Pathology Department's configured PCs were used as client PCs.
Client PC1: 10MB/s network connection, 2GB Memory

Client PC2: 100 MB/s network connection, 1GB Memory
All viewers were an open HTTP message interface to enable client software to incrementally access image information and view data from virtual slides.
Images were located in the storage server, in the Imaging Lab's network storage and on three outside servers. Applications were for basic view, 3D reconstruction, and multilayer (9 layers).

One of the four WSI systems used JPEG2000 as the compression algorithm. The other three used JPEG. View size for all was 1280x1024 pixels.

1. Basic viewer

The time to data completion was measured at seven conditions. All data were an average of three measurements.
1. open an image, 2. change to 40x view, 3,4,5. change the coordinates of current view. 6. change to 5x, 7. change to 1.25x

2. JPEG 2000 performance measurement

3. 3D reconstruction
100 serial sections of WSI were used. The time to complete the 3D model was measured.

4. Multilayer

Results

Tables 1-4 show the results of the study. Table 1 shows the time taken (seconds) to complete the data transfer of basic viewing function at seven different conditions.

Table 1
1.1. Image 1: image size is 18GB, file size is 667M

	a, A	a, B	b, A	b, B
1	3	2	2	3
2	2	2	1	1
3	1.5	1.5	1	1
4	2	1.5	1	1
5	2	1.5	1	1
6	3	3	2	2
7	9	7	7	7

1.2. Image 2: image size 39.7GB. file size 2.2GB

	a, A	a, B	b, A	b, B	a, C2	b, C2
1	7	6	2	2	7	11
2	4	4	1	1	7	7
3	3	2	1	1	3	2
4	2	2	1	1	3	3
5	3	2	1	1	3	3
6	3	3	2	2	7	6
7	15	10	7	7	4	4

Table 2. JPEG 2000, Image size 24GB, file size 1.6.GB

	a, C1	b, C1
1	30	31
2	7	16
3	3	9
4	3	9
5	2	10
6	24	55
7	27	62

Table 3. 3D reconstruction: 100 of 500-600 MB/file, each image size 3.5 GB.

	a, B	b, B
Load all images	86	66
Complete reconstruction	250	126

Table 4. Multilayer
A Cytology specimen of nine layers WSI was used. [and ease of viewing at the different focus plane was assessed.]
Size of specimen: 10mm2, file size 2.56GB, Image size 105GB

	a, A	a, B	b, A	b, B
1	15	15	<1	<1
2	3	7	<1	<1
3	1	1	<1	<1
4	1	2	<1	<1
5	1	2	<1	<1
6	5	7	<1	<1
7	2	2	<1	<1
Change Layer	1/layer	1-1.5/layer	<1	<1

*1. open an image, 2. change to 40x view, 3,4,5. change the coordinates of current view. 6. change to 5x, 7. change to 1.25x. a. Client PC was 10MB/s with 2GB Memory, b. client PC was 100MB/s with 1GB memory, A. Image in Network hard drive B image was in the hard drive of storage server, C1-C3. image was the server outside MGH the unit of the data was second

Discussion

Our findings were quite interesting.

- The amount of computer memory is more important than network speed when images are accessed externally via the internet. Computer memory is also more important when images are accessed with JEPG2000
- Network speed is more important when images are accessed locally through the intranet.
- On some of the viewers it took more than three minutes for the images to load when accessed from an outside server via the internet, an unreasonable amount of time for any user to wait.
- An external hard drive could be useful. However, the particular network conjunctions still might affect the speed at which images could be accessed.

Our network conditions are not yet ideal for many reasons, including budgetary constraints, institutional policy, etc. We built our own WSI network/server system without the support of internal network specialists. The data we have been collecting will be very useful when we begin planning upgrades to our WSI network/server with out network specialist.

Conclusion

Many more of our stored images will be accessible externally in the near future, and we will continue investigating network, storage and data format issues. In the meantime, it is clear that successful implementation of WSI for multiple uses depends on more than the scanner itself, and that all network and storage components must be studied and evaluated.

Virtual Microscopy in a Developing Country: A Collaborative Approach to Building an Image Library

Erick Ducut[1], Fang Liu[1], Jose Ma. Avila[2], Michelle Anne Encinas[2], Michele Diwa[2] and Paul Fontelo[1]

Office of High Performance Computing and Communication, National Library of Medicine[1]
Department of Pathology, University of the Philippines Manila College of Medicine[2]
email: pfontelo@mail.nih.gov

***Abstract*— Virtual microscopy is the process of digitally acquiring microscopic glass slides. The product, a "virtual slide", becomes a digital representation of the microscopic glass slide. Virtual microscopy is an inevitable and expected technological development in the teaching of histopathology in medical schools. However, for medical schools in low-resource countries with developing economies, this advancement might prove difficult and trying especially with their limited resources. One way to address this problem is to form collaborative projects with educational institutions in developed countries. Medical schools in the developed countries in turn can expand their virtual image collection by augmenting it with histopathologic slides from developing countries. We demonstrate this collaborative approach of developing a virtual slide collection using an institution's own glass slide collection and making it available on the Internet for teaching.**

***Index Terms*—Virtual microscopy, virtual slide, digital pathology, digital image.**

I. INTRODUCTION

Since the beginning, medical histology and pathology have been part of the medical curriculum worldwide. Traditionally, these courses are taught using a set of microscopic glass slides viewed under the optical microscope. In an ideal situation, students have their own individual microscope and they are available anytime of the day. Sadly, in developing countries, the cost of acquiring and maintaining light microscopes and constantly replacing broken slides is high. Depending on a medical school's resources, medical students may have their own microscope or they may have to share it with one or more students. Sharing microscopes and using poorly maintained equipment does not lead to an optimal learning environment.

Virtual microscopy is the process of digitally acquiring microscopic glass slides. The product, a "virtual slide", becomes a digital representation of the microscopic glass slide. A virtual microscope simulates the experience of examining a glass slide under a light microscope [1], [2]. With advances in image acquisition and storage, virtual microscopy is revolutionizing the teaching of histology, pathology and other related disciplines. Furthermore, recent innovations in image compression and delivery over the Web make it an ideal tool for teaching at a distance and for the practice of telemedicine. With virtual microscopy, resources can be shared with other students worldwide.

Unlike traditional light microscopy, virtual images of an entire histopathologic specimen can be viewed on a monitor and allow multiple viewers to see the images simultaneously at different locations. Aside from equal access by every student, this promotes a collaborative environment and enhances discussion and learning. Images can also be viewed anywhere thus maximizing a student's study time. Moreover, digitized images can be archived on a network server and can be shared with other schools especially those areas with low access. Unique or rare medical cases can be shared with hospitals and schools where these types of cases are rarely encountered. Lastly, virtual microscopy will allow medical schools to avoid the cost of purchasing and maintaining optical microscopes and glass slide collections. This allows them to allocate the funds for other uses [1].

In 2005, Fontelo, et. al evaluated the diagnostic accuracy of a virtual microscopy set-up using surgical pathology specimens in a university hospital setting. In their paper, the authors discussed the potential application of this technology in augmenting medical education and telemedicine in low-resource countries [1]. The main objective of our present project was to demonstrate this collaborative approach of developing a virtual slide collection using the institution's own glass slide collection and making it available on the Internet for teaching. The project was done as a collaborative project between the Department of Pathology, University of the Philippines College of Medicine (UPCM) in Manila and the Office of High Performance Computing and Communications, National Library of Medicine (NLM). The glass slides, part of the current first and second year pathology course teaching set, were sent by courier then digitized at the NLM. The virtual slides are hosted in a Web server at the National Library of Medicine.

II. METHODS

A. Slide Acquisition

Pathology teaching glass slides, stained with hematoxylin and eosin stains were selected for digitization and were sent to the study proponents at the National Library of Medicine. All patient information was removed from the glass slides.

B. Slide Scanning

Each glass slide was cleaned and prepared for scanning. Image acquisition was done using the Aperio ScanScope T3 Slide Scanning System [3]. This scanning system can digitize an entire microscope glass slides at gigapixel resolution, producing true-color, seamless virtual slide images. Five slides can be loaded simultaneously. Digital images produced by the scan system were recorded in a lossless compression format, the Tagged Image File Format (tiff) with a ScanScope Virtual Slide (.svs) extension.

C. Image Digitization and Web Rendering

Using the Aperio Digital Slide Studio, each .svs image file was compressed to the Joint Photographic Experts Group (jpeg) format [4]. The software integrates flexible image adjustment and export capabilities with digital slide viewing. Software functions include zoom, crop, rotate, scale, adjust brightness and contrast, apply digital filters, add/delete, thumbnail and label images, and recompress images into other common file formats.

Each JPEG file was then processed using Zoomify, a tool to make images 'zoomable' [5]. Zoomify processes an image by “slicing” it into many high quality pieces or tiles. The application performs this action on many versions of the image, each at a different resolution, resulting in a pyramid of tiles that can be used to navigate and view any part of the image at any “magnification” level. Web viewing is fast and interactive and no special software is needed as Zoomify uses JPEG, HTML, and a Flash plug-in as the Web 'viewer' [5].

A Web browser interface was developed using PHP and MySQL. Clicking on each of the link in the interface will show the respective virtual image (Figure 1). Images can be viewed in higher magnification just by clicking on an area in the image (Figure 2). Images can be panned in all directions by hold-clicking the image and moving the mouse to the desired direction. A thumbnail image next to the large image provides navigation landmarks to orient the user. This simulates viewing the glass slides under a light microscope. Instructions are provided in the index page and navigation buttons are included in the image frames.

D. Educator/Student Evaluation

The Department of Pathology of the University of the Philippines Manila, College of Medicine used the

Fig 1. Screenshot of a scanning view of a virtual slide.

interface to augment teaching to their medical students and residents (Figure 3). Evaluation of the program

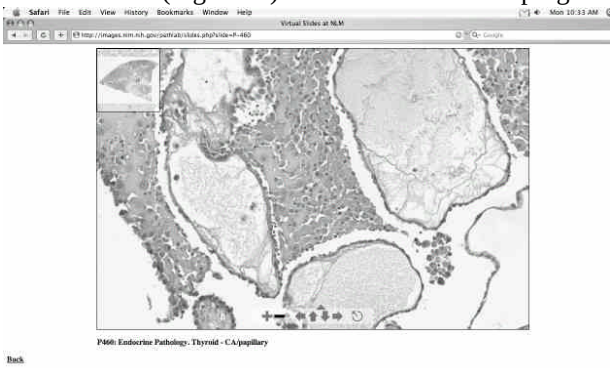

Fig 2. Screenshot of a magnified view of a virtual slide.

included ease of use of the interface, quality of the images, and Web access and its limitation. Both educators and students provided feedback on the usability of the program in their medical training.

III. RESULTS

After necessary approvals from the regulatory board of the Philippine General Hospital, the teaching hospital of

Fig 3. A Pathology instructor in the Department of Pathology, University of the Philippines College of Medicine using the virtual slide collection to discuss clinical cases with medical students and residents

the University of the Philippines Manila College of Medicine, Department of Pathology, 20 histopathologic

glass sides were shipped to the National Library of Medicine for inclusion in the project. Each glass slide was part of the teaching collection in histopathology of the department and is similar to the set of slides that are loaned to the students at the start of the school year.

Digital images produced by the scanning system were recorded in the Tagged Image File Format (tiff) with a ScanScope Virtual Slide (.svs) extension. Final file size ranged from 23 megabytes to 560 megabytes with an average size of 341 megabytes.

Department of Pathology instructors and professors from the University of the Philippines Manila College of Medicine accessed the Web interface to augment their teaching materials to medical students and hospital residents. Using a desktop or laptop computer connected to the Internet, they projected the virtual slides and demonstrated to the students how the entire experience of using a light microscope can be simulated using the virtual microscope.

A formal evaluation using satisfaction surveys is currently being undertaken. Initial feedback shows that faculty members and students rate the technology highly. One issue shared by the teachers concerned the inadequacy of the present school system's Internet set-up and speed to load the images in a timely fashion.

Pathology teaching glass slides, stained with hematoxylin and eosin stains were selected for digitization and were sent to the study proponents at the National Library of Medicine. All patient information was removed from the glass slides.

IV. DISCUSSION

The curriculum of medical schools worldwide has undergone significant changes in the past few years. These changes have focused on reducing teacher-student contact hours to decompress crowded programs, increasing emphasis on independent learning, and development of interpersonal and problem solving skills. In this changed environment, many strategies have been employed to improve student experience in learning. Current modes of medical instruction utilize student-centered experiential learning, research reflection and collaborative activities [6].

With significant technological developments in computing, recent trends in medical education have been to incorporate computers into both instruction and independent study. One of these trends is to shift from the use of glass slides to virtual microscopy images. Whereas before, students were loaned a collection of glass slides that they reviewed under a light microscope, guided by their textbook atlas and augmented by their teacher's lecture, developments in image acquisition and digitization have allowed medical schools to develop a collection of virtual images that students can access on their own or as a group. Mimicking the experience of using a light microscope, these virtual images can be scanned by moving the computer mouse to the direction they wish to pan. Clicking on the images can increase or decrease magnification and simulate changing the resolutions in a light microscope [7].

Virtual microscopy offers a unique set of advantages over traditional light microscopy. Virtual slides always remain in focus, with ideal condenser and light settings, thus decreasing student effort and some of the frustrations in operating a real light microscope [8]. Even at higher magnifications, students are able to maintain orientation with respect to the entire histopathologic specimen. Since students have access to the same set of slides, student complaints that their set of glass slides are not as good as those of a fellow student is eliminated completely [9].

Unlike traditional light microscopy, virtual images of an entire histopathologic specimen can be viewed on a monitor and allow multiple viewers to see the images at the same time. And since virtual images can be viewed simultaneously by several students, discussion of the structures of interest in the virtual slides is facilitated and questions can be easily addressed by both the teacher and the students [1]. An instructor's time is used more efficiently – instead of shuttling between student to student to look at the microscope, the entire class or group can view the image simultaneously. Questions are answered for all to hear and learning is enhanced. This promotes a collaborative environment and promotes discussion.

Virtual images may be standardized and archived for instruction, performance evaluation and research. Faculty members appreciate the ease of using the virtual slides for examinations [9].

Digital images can also be viewed anywhere and anytime thus augmenting a student's individual study time. This approach can allow a decrease in the faculty to student ratio in the laboratory without compromising educational experience of the medical students [9].

Virtual microscopy provides the ability to increase the number of virtual slides in any medical school's collection by sharing digital images with other institutions [9]. Digitized images can be archived on a network server and can be shared to other schools especially those with low access to resources. Unique or rare medical cases can be shared to rural hospitals and schools who normally would not see such cases [1].

Some students are reportedly hesitant to use microscope glass slides for fear of breaking them and incurring replacement costs [7]. With virtual microscopy, the cost of maintaining a collection of glass slides for each of the medical students is thus eliminated. Virtual microscopy also allows medical schools to avoid the cost of purchasing and maintaining the traditional microscopes and encourage them to allocate the funds for other pressing matters. Lastly, physical space will no longer be as essential to store light microscopes and glass slide collections [7].

In several reports, medical educators and students have rated virtual microscopy very high in terms of its effectiveness for learning. A large majority of students indicate that they prefer learning via a virtual microscope

to the light microscope [6], [7]. Reports also showed that virtual microscopy improved the difference between the students' pre- and post-laboratory test scores and has augmented student learning efficiency by reducing the amount of time spent on laboratory sessions. These emphasize the fact that virtual microscopy can be a viable addition to, if not a potential replacement for, real light microscopes and glass slides in teaching histopathology [8].

Faculty members with extensive previous experience using the light microscope were interviewed and asked if they prefer teaching with the light microscope or virtual microscope. Nearly all of them indicated a strong preference for using the virtual images.[7] They reported that the capability to simultaneously view a virtual image on a single computer monitor to discuss structures of interest is a distinct advantage of virtual microscopy and significantly increases teaching efficiency in histolopathology laboratories. They are also pleasantly surprised to find evidence of active and independent student learning, as well as the extent to which the students were open to undertake collaborative group work [6].

Unfortunately, medical schools in low resource countries with developing economies still have to adopt this new technology. The high initial cost to procure and maintain the scanner prohibits medical schools with limited resources to transition from using light microscopes and glass slides to virtual microscopy. One way to circumvent this obstacle is to form collaborations with learning institutions in developed countries. Most institutions might be willing to work on a project with other schools especially if it would also add to their own collection of virtual images. Schools with limited resources in turn would receive the same content for teaching as their counterparts in developed countries.

The Department of Pathology of the University of the Philippines Manila College of Medicine used the virtual library created to supplement the teaching of pathology to its students and the residents of the Philippine General Hospital, its teaching hospital. Though a formal evaluation is still forthcoming, initial feedback among faculty and student are very favorable. One problem mentioned by the educators concerned the inadequacy of the present school system's Internet set-up and speed to load the images in timely fashion. One suggestion made to address this problem is to archive the virtual images to a local intranet server.

V. CONCLUSION

Virtual microscopy is an inevitable and expected technological development in the teaching of histopathology in medical schools. However, for medical schools in low-resource countries with developing economies, this advancement might prove difficult and trying especially with their limited resources. One way to address this problem is to form collaborative projects with educational institutions in developed countries. Medical schools in the developed countries in turn can expand their virtual image collection by augmenting it with histopathologic slides from developing countries. Our project was able to demonstrate this concept is very much feasible and in the long run will prove beneficial for both parties.

ACKNOWLEDGMENT

This research was supported by the Intramural Research Program of the National Institutes of Health (NIH), National Library of Medicine (NLM), and Lister Hill National Center for Biomedical Communications (LHNCBC).

REFERENCES

[1] P. Fontelo , E. DiNino , K. Johansen , A. Khan and M. Ackerman, "Virtual microscopy: Potential applications in medical education and telemedicine in countries with developing economies," *Proc 38th Hawaii Int Conf Sys Sci*, 2005.

[2] R. Conran, P. Fontelo, F. Liu, M. Fontelo, E. White, "Slide2Go: A virtual slide collection for pathology education," *AMIA Annu Symp Proc*, vol. 337, 2007, p. 918.

[3] Aperio: Bringing Digital Pathology to Life. Available: http://www.aperio.com/

[4] Spectrum Functionality: Digital Slide Studio. Available: http://www.aperio.com/pathology-services/digital-slide-studio-edit-export.asp

[5] Zoomify – Zoomable web images! Available: http://www.zoomify.com/

[6] R.K. Kumar, B. Freeman, G. M. Velan and P.J. De Permentier, "Integrating histology and histopathology teaching in practical classes using virtual slides," *Anat Rec*, vol. 289B, pp. 128-133.

[7] B.B. Krippendorf and J. Lough, "Complete and rapid switch from light microscopy to virtual microscopy for teaching medical histology," *Anat Rec*, vol. 285B, pp. 9-25.

[8] T. Harris, T. Leaven, P. Heidger, C. Kreiter, J. Duncan and F. Dick, "Comparison of a virtual microscope laboratory to a regular microscope laboratory for teaching histology," *Anat Rec*, vol. 265, pp.10-14.

[9] C.A. Blake, H.A. Lavoie and C.F. Millette, "Teaching medical histology at the University of South Carolina School of Medicine: Transition to virtual slides and virtual microscopes," *Anat Rec*, vol. 275B, pp. 196-206.